Redox-Flow Batteries: From Metals to Organic Redox-Active Materials

Jan Winsberg[+], Tino Hagemann[+], Tobias Janoschka, Martin D. Hager, and Ulrich S. Schubert*

Keywords:
electrochemistry · energy storage ·
organic active materials ·
organic electrolytes ·
redox-flow batteries

Angewandte
International Edition *Chemie*

Research on redox-flow batteries (RFBs) is currently experiencing a significant upturn, stimulated by the growing need to store increasing quantities of sustainably generated electrical energy. RFBs are promising candidates for the creation of smart grids, particularly when combined with photovoltaics and wind farms. To achieve the goal of "green", safe, and cost-efficient energy storage, research has shifted from metal-based materials to organic active materials in recent years. This Review presents an overview of various flow-battery systems. Relevant studies concerning their history are discussed as well as their development over the last few years from the classical inorganic, to organic/inorganic, to RFBs with organic redox-active cathode and anode materials. Available technologies are analyzed in terms of their technical, economic, and environmental aspects; the advantages and limitations of these systems are also discussed. Further technological challenges and prospective research possibilities are highlighted.

From the Contents

1. Introduction

The global energy demand is fulfilled mainly by the production of electricity from fossil fuel and nuclear-based power plants. These conventional energy production plants have typical power outputs of over 1 GW, but are far from being sustainable. Fossil fuels have been exploited on a large scale since the start of the industrial revolution in the 19th century.[1] Since then, the concentration of carbon dioxide in the atmosphere has increased from 280 ppm to over 401 ppm in December 2015.[2] CO_2, as well as other greenhouse gases, seems to be the main origin of climate change.[3–5] Additionally, coal-fired power plants emit a multitude of different toxic heavy metals and fine dust.[6,7] Although nuclear power plants were once proposed to be the main alternative to fossil fuel based plants to reduce CO_2 emissions but, from the point-of-view of a responsibly acting society, they should not be utilized for electricity generation.[8–11] In fact, we need to change our energy production to "green" and renewable sources, such as geothermal and solar energy, hydroelectricity, and wind power. However, geothermal energy and hydro-electricity are associated with other disadvantages (e.g. limited availability or massive ecological impact) and are limited to certain geographical conditions.[12,13] The utilization of solar energy and wind power, thus, seems to be the most promising alternative.[14,15]

A large number of new power plants using solar energy and wind power were built in the last few years throughout the world and a major expansion is planned until 2020 and 2050, respectively.[16] Furthermore, a second trend to local small-scale energy production by photovoltaics is recognizable.[17] Unlike before, electricity is now generated discontinuously—depending on the weather—and in a more decentralized manner, often on a kW scale. Today's electricity grids are not designed for this kind of energy production.[18] Conventional power plants produce a stable base load over a long period of time. In contrast, energy production from wind power and solar energy is intermittent and energy demand can diverge from energy production. Intelligent storage technologies are required to overcome temporal deviations in energy production and consumption.[19] Only with the combination of renewable power sources and energy storage systems, connected as a smart grid, can the turn-around in energy policy ("Energiewende") be successful.[20]

Possible storage technologies are pumped hydro, compressed air, thermal, flywheel, superconducting magnetic, electric double layer, and electrochemical energy storage systems.[21] Typical sizes of photovoltaics range between 1 kW (small-scale roof-top system) up to 550 MW (Topaz Solar Farm, California, USA), and wind turbines typically produce a power of 2.5 MW (up to even 7.5 MW for the newest generation of large wind turbines). With this power range in mind, RFBs seem to be an ideal storage technology for wind and solar electricity.

[*] J. Winsberg,[+] T. Hagemann,[+] T. Janoschka, Dr. M. D. Hager, Prof. Dr. U. S. Schubert
Lehrstuhl für Organische und Makromolekulare Chemie (IOMC)
Friedrich-Schiller-Universität Jena
Humboldtstrasse 10, 07743 Jena (Germany)
E-mail: ulrich.schubert@uni-jena.de

J. Winsberg,[+] T. Hagemann,[+] T. Janoschka, Dr. M. D. Hager, Prof. Dr. U. S. Schubert
Center for Energy and Environmental Chemistry Jena (CEEC Jena)
Friedrich-Schiller-Universität Jena
Philosophenweg 7a, 07743 Jena (Germany)

[+] These authors contributed equally to this work.

2. General Principles of Flow Batteries

The central components of redox-flow batteries are an electrochemical cell and two tanks. The electrochemical cell contains two electrodes and a separator. An electrolyte solution is circulated between these components by pumps. The redox-active cathode and anode materials are not formed as solid electrodes, but are dissolved in the electrolyte, for which reason it is named as either the catholyte or anolyte. The separator is permeable to the supporting electrolyte (a conducting salt), but impermeable to the redox-active material. This setup, similar to fuel cells, enables the power and capacity of the battery to be scaled independently from each other. A schematic representation is provided in Figure 1a. A hybrid-flow battery (HFB) is a similar type of flow battery. It features at least one redox couple with a solid redox state (Figure 1b). This active material is electroplated on an electrode during charging and dissolved again in the electrolyte in the subsequent discharging process. This cell design must be adopted, as the electroplated metal often forms dendritic structures, which may cause a short-circuit or puncture the membrane.[22]

The electrical performance of the battery is affected by many parameters and can be measured by the following benchmarks. The volumetric capacity of the electrolyte indicates the amount of charge that can be stored in a certain amount of electrolyte [Eq. (1)]. The redox-active material can

$$C = \frac{m \cdot n \cdot F}{M \cdot V} \tag{1}$$

be dissolved, but particles, gases, or ionic liquids can also be utilized. Thus, the volumetric capacity is dependent on the amount of redox-active material and the number of electrons that participate in the redox process. The unit most used for the volumetric capacity is $Ah L^{-1}$. The energy density includes the voltage between the utilized redox couples and is, thus, measured in $Wh L^{-1}$ [Eq. (2)].

$$E = C \cdot U \tag{2}$$

C = volumetric capacity, m = mass, n = number of electrons, F = Faraday's constant, M = molar mass, V = volume, E = energy density, and U = voltage.

Jan Winsberg studied Business Chemistry at the Heinrich Heine University Düsseldorf, Germany, where he obtained his BSc and MSc in the field of macromolecular chemistry. He joined the group of Prof. Schubert as a PhD student in 2013, where he develops organic redox-active materials for redox-flow batteries.

Tino Hagemann studied Chemistry at the Friedrich Schiller University Jena, Germany. He obtained his diploma in chemistry in the field of complex chemistry and in 2013 he joined the group of Prof. Schubert as a PhD student, where he develops organic electrolytes for redox-flow batteries.

Tobias Janoschka studied Chemistry and Business Administration at the Friedrich Schiller University in Jena, Germany. He joined the group of Prof. Schubert as a PhD student in 2011 with a scholarship from the "Fonds der Chemischen Industrie", specializing in organic and macromolecular synthesis. His current focus is on innovative electroactive materials for redox-flow batteries.

Martin D. Hager completed his PhD in 2007 at the Friedrich Schiller University Jena in the group of Prof. Dr. Elisabeth Klemm, working on conjugated (rod-coil) polymers for polymer solar cells. After postdoctoral research at the TU Eindhoven, in 2008 he became a group leader in the group of Prof. Schubert at the FSU Jena. His research interests include reversible polymer systems for self-healing applications, conjugated polymers for solar cells, as well as redox-active polymers for batteries (from small printable devices to large redox-flow-batteries).

Ulrich S. Schubert was born in Tübingen (Germany) in 1969. He studied chemistry in Frankfurt and Bayreuth (Germany) and at the Virginia Commonwealth University, Richmond (USA). His PhD was performed at the Universities of Bayreuth and South Florida. After postdoctoral research with Prof. J.-M. Lehn at the University of Strasbourg (France), he moved to the TU Munich (Germany), where he habilitated in 1999. From 1999 to 2000 he was Professor at the University of Munich, and from 2000 to 2007 Full Professor at the TU Eindhoven. Since 2007, he has been a Full Professor at the Friedrich Schiller University Jena.
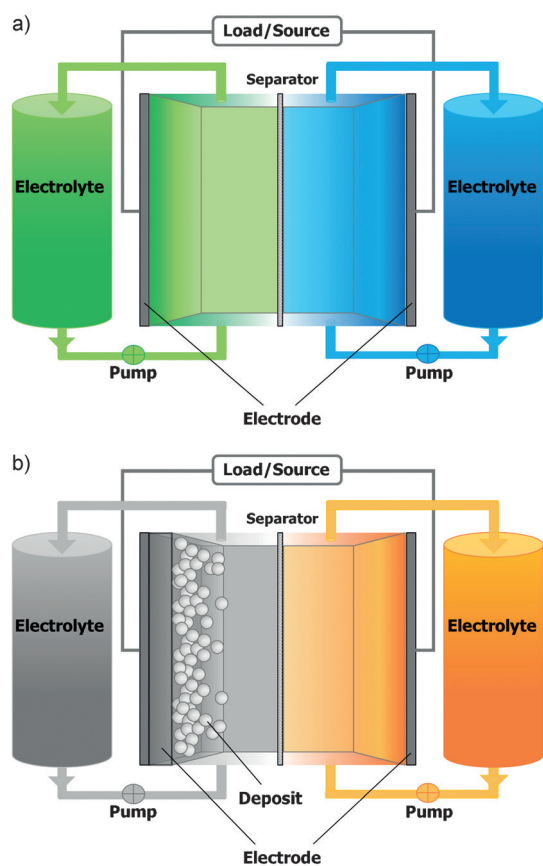
Figure 1. a) Schematic representation of a redox-flow battery (RFB). The battery consists of an electrochemical cell with two compartments and a separator in between. The electrolyte is circulated between the cell and the storage tanks by pumps. b) Schematic representation of a hybrid-flow battery (HFB). A material is electroplated in the charging process on one electrode.

The current density has a direct impact on the charging/discharging time of the battery, and is related to the membrane area of the electrochemical cell. An often used unit is $mA\,cm^{-2}$, which translates to power density $mW\,cm^{-2}$ if the voltage is taken into account.

The coulombic efficiency (CE), sometimes referred to as the faradaic or current efficiency, and the voltage efficiency (VE) are two important indicators of the electrical quality of a flow battery. The CE relates the charge applied in the charging procedure to the retained charge in the discharging procedure of the same charge/discharge cycle [Eq. (3)].

$$CE = \eta_C = \frac{Q_D}{Q_C} \tag{3}$$

Coulombic efficiencies $< 99\%$ are an indication of crossover of the redox-active material through the membrane into the opposite half-cell or irreversible side reactions of the redox-active material or the electrolyte itself, for example, hydrogen formation.

$$VE = \eta_V = \frac{\frac{\int_0^{T_D} E_D(t)dt}{T_D}}{\frac{\int_0^{T_C} E_C(t)dt}{T_C}} = \frac{\bar{E}_D}{\bar{E}_C} \tag{4}$$

$$EE = \eta_{EE} = \eta_C \cdot \eta_V \tag{5}$$

$\eta =$ efficiency, subscripts: $C =$ charging, $D =$ discharging, $Q =$ charge, $T =$ time for charging/discharging, and $E =$ potential.

VE is the ratio between the mean discharging voltage and the mean charging voltage at constant current [Eq. (4)]. The difference between these mean values is caused by a variety of overpotentials. The diffusion, polarization, and ohmic overpotential are decisive for flow batteries.[23–25] The VE decreases as the current density increases. The multiplication of CE by VE yields the energy efficiency [EE; Eq. (5)], which is a measure of the applied and retained energy. Typical EE values of RFBs are in the range of 50 to 90%, depending on the applied current density and material quality.

2.1. Redox-Active Materials

The redox-active charge-storage material has a significant impact on the performance of a flow battery. Its reaction kinetics have an influence on the applicable current density, and the viscosity of the electrolyte is also affected by the redox-active material and its concentration. A general decrease in performance can be observed at higher viscosities, as the charge-carrier mobility within the electrolyte is reduced and the energy requirement for electrolyte circulation is increased. The employed active materials are often metal-based redox couples dissolved in aqueous media, but a greatly increasing number of charge-storage materials based on organic redox-active molecules have been reported recently.[199,200] Some of these organic materials are not soluble in water and, thus, the utilization of an organic solvent is required. Organic aprotic solvents show a better electrochemical stability and a wider potential window than protic solvents such as water. This can lead to batteries with higher energy densities, as redox couples with an elevated voltage can be used. However, the ion conductivity in organic solvents is much lower, which limits applicable current densities. This effect is partially mitigated by a higher voltage (power density). Some organic materials are soluble in water, particularly if the molecule contains polar substituents. Thus, high current densities are applicable, but the voltage between the two redox couples is restricted. Hence, an "L" shape in Figure 2 is clearly visible, which illustrates the limitations of current flow-battery technologies.

A variety of organic molecules have been investigated as charge-storage materials in polymer-based organic batteries, for example, stable NO radicals, carbonyl compounds, and organosulfur compounds.[26] These studies can be used as the starting point for the development of suitable organic materials tailored for applications in RFBs. These materials, which can be obtained by synthetic approaches, have to feature at least two stable and (electro)chemically reversible redox states. Starting materials can be obtained from petrochemistry or, in the best case, by extraction from renewable
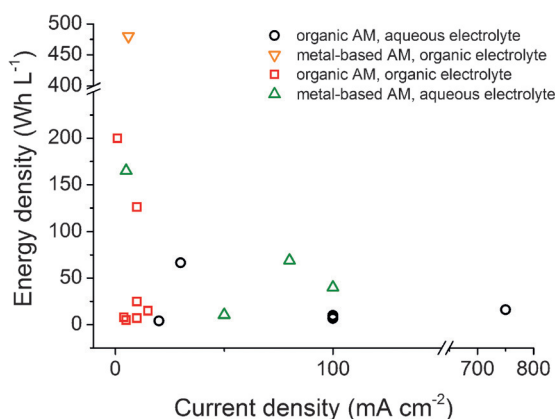
Figure 2. Energy density versus current density of selected RFB systems (AM = active material).

sources, white biotechnology, as well as in the future by power-to-X technologies. Nevertheless, the exploitation of organic starting materials is not limited to certain geographical areas, but can be performed globally if an independent procurement of organic raw materials is possible. In particular, Europe, being poor in numerous critical raw materials, might profit from its strong chemical industry, which can produce organic active materials on a large scale. Another advantage is the flexibility of organic materials. Solubility, chemical reversibility, and redox potential can be tuned by modification of the organic core component with particular functional groups to improve the battery performance. The reversibility of the utilized redox couples are of particular interest, since the (electro)chemical reversibility determines the number of possible charge/discharge cycles of a flow battery.

2.2. Separators

An ideal separator of a flow battery keeps the redox-active couples completely apart, but is permeable to the supporting electrolyte ions to enable charge balance.[27] The selectivity of the separator is crucial, as a cross-contamination of catholyte and anolyte leads to reduced efficiencies and, in the case of asymmetric electrolytes, a long-term decay of capacity.[28] A limited number of flow batteries can be used without a separator, for example, flow batteries with two solid electrodes or batteries with a gas diffusion electrode.[29,30] A wide range of separators were investigated over the last few years: perfluorinated and non-perfluorinated ion-exchange membranes (e.g. Nafion) are often used.[31] In flow batteries, where solvated polymeric species or particles are the utilized active material, porous separators, such as dialysis membranes or simple microporous PP/PE foils, can be used.[32–37] Furthermore, the modification of polymer-based membranes with coatings of inorganic particles, for example, was reported to increase the selectivity of the separator.[38]

A low resistance of the separator is essential for good performance parameters of the battery. The mechanical firmness and chemical inertness are of great importance for

the long-term performance stability.[39] The "fouling" of a membrane gradually reduces the performance values of an RFB. It develops by attractive interactions between the membrane and the electrolyte, which causes an accumulation of these compounds on the surface or within the pores of the membrane. This can lead to reduced selectivity (retention of the active materials) up to the point of complete clogging of the separator.[40]

Flow batteries with different solvents for the anolyte and catholyte require the utilization of separators that completely isolate the two compartments, for example, Li in propylene carbonate (anolyte) and TEMPO in water (catholyte). Ceramic membranes, which are conductive for a single ion, are utilized for this purpose. A significant drawback of this membrane technology is the restricted ion conductivity, which leads to limited applicable current densities.[41]

2.3. Electrodes

The electrodes of RFBs do not take part in the redox reactions of the cathode- and anode-active material, but provide the active surface for the reactions of the redox couples dissolved in the catholyte and anolyte, respectively. They have to feature an excellent electrical conductivity,[42] high specific surface area, stability in the applied operating potential range of the RFB, and chemical inertness against the often highly corrosive electrolytes.[43,44] The corrosion process of an electrode—for example, CO_2 evolution in all-vanadium RFBs—decreases the performance characteristics of the electrode.[44–46] In addition, electrodes should facilitate a good wettability of the electrolyte and enable high reaction kinetics of the utilized redox couples. Depending on the applied active material, this can be accomplished by activation or modification of the electrode by oxidation, doping, or addition of nanomaterials.[47–56] Solutions of organic compounds in water show a surfactant-like behavior and a low surface tension. This results in a good wettability behavior, even without electrode modification.[34] Frequently used electrodes are graphite felt and carbon paper, but advanced electrodes were also fabricated from, for example, carbon nanotubes, which catalyze the redox reactions.[57] Electrodes consisting of metal mesh/foam are also used and can be coated with, for example, platinized Ti or IrO_2.[58–60] A common side reaction during operation of aqueous batteries is the water-splitting reaction. An ideal electrode utilized in aqueous-based electrolytes prevents the evolution of hydrogen and oxygen, which is a main cause for charge imbalance and efficiency losses. However, hydrogen evolution is not limited to aqueous electrolytes, but is possible in all protic solvents. For example, Suarez et al. reported sufficient inhibition of H_2 generation on a graphite felt electrode that was coated with Bi nanoparticles.[61] This effect is accompanied with a slightly shifted potential of the vanadium reduction to higher potentials; presumably caused by a catalytic effect. However, the optimization of the electrodes has been investigated only for inorganic active materials. Therefore, there is a great need for research to optimize the electrodes for organic active materials.

2.4. Advantages and Challenges of Flow Batteries

Flow batteries offer a variety of benefits. The power and capacity of the system can be scaled independently from each other by separate sizing of the tank volume and the cell stacks (reaction cells). This allows an exact adaption to the associated generator unit. Flow batteries can switch between charging and discharging within a fraction of a second, but are actually designed for storing electricity for several hours.[21] In addition, modularized flow batteries, in the form of shipping containers, can be moved and set up as "mobile" energy-storage devices.[62] In this way, the electrical power supply in decentralized regions, for example in developing countries, could be ensured.[17] Common flow batteries rely on aqueous electrolytes that are not flammable, and a safe battery operation is guaranteed. The lifetime exceeds that of lead-acid and lithium ion/polymer batteries significantly. These advantages can be utilized for application possibilities, such as, peak shaving, as well as load and frequency balancing.[63] The increasing amount of electricity generated from renewable sources, such as wind power and solar energy, can lead to peaks in the energy production. For example, a significant increase in electricity produced from photovoltaics is observable around midday. In contrast, the energy demand is relatively low at this time compared to the evening. Electricity production from wind energy can exceed the energy demand considerably in stormy periods.[64] These phenomena can be monitored in the energy profile.[65–68] Flow batteries can be used to flatten these profiles (peak shaving). When viewing the system as a whole, large energy-storage devices reduce the risk of black-outs caused by net frequency exceedances by intercepting over-production.[64,69] For this purpose, enormous energy-storage devices have to be developed that have lifetimes of at least 20 years, to offer cost-efficient and reliable energy storage. In contrast to the proof-of-principle small-scale flow batteries, these large-scale systems are operated in a different manner. Whereas laboratory-scale tests are often performed under extreme conditions to study the material's properties, practical applications rely on milder conditions to extend the material's lifetime. Large-scale systems have to deal with the hydraulic and electric cascading of numerous cell stacks and intelligent battery management systems. The development effort for these complex systems is very high, since a variety of components and peripheral devices have to be harmonized and coordinated.[70] Further challenges are the relatively low volumetric energy density compared to lithium ion/polymer and lead-acid batteries. Current commercially available all-vanadium RFB (VRFB) systems feature an energy density of 25 Wh L^{-1},[71] with conventional storage technologies such as lead-acid (40 Wh kg^{-1}, 100 Wh L^{-1}) and lithium ion/polymer (180 Wh kg^{-1}, 100 Wh L^{-1}) easily outperforming this value.[72] Hence, the space requirement of flow batteries is rather large to be competitive in the field of overall capacity. However, flow batteries have a better volumetric capacity than pumped hydro storage, the technology mostly used in the USA.[73]

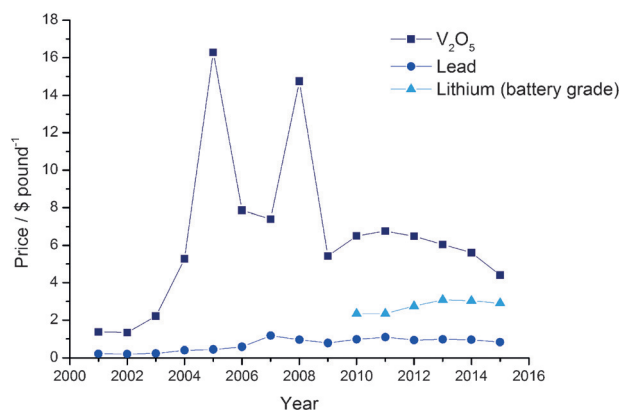The acquisition and working costs are one of the most significant drivers that determines market penetration. The

Figure 3. Commodity prices of Li (battery grade), Pb, and V$_2$O$_5$ (standard grade). Data obtained from the U.S. geological survey.

commodity price of vanadium is strongly dependent on the amount of high-performance steel produced and is, relatively high compared to lead and lithium (Figure 3). Additionally, a remarkable fluctuation was observed between 2004 and 2009, which can be expected to recur with new economic growth in China within the next few years.

The Advanced Research Projects Agency-Energy (ARPA-E) of the Department of Energy (DOE) set a capital cost target of $100 kW^{-1}h^{-1} for one hour of storage for market penetration.[74] An important advantage of RFBs that utilize organic charge-storage materials is a possible cost benefit over metal-based RFBs. Several cost analyses were performed, amongst others, by Darling et al. that illustrate that the two primary cost drivers are the price of the active material itself and the price of the utilized membrane.[75–77] As a consequence, the production costs for the organic active material have to be as low as possible. This requires low-cost starting materials, simple chemical reactions with full conversion, and no necessary purification steps. A basic calculation was performed by Huskinson et al., which found redox-active material prices of $27 kW^{-1}h^{-1} for the anthraquinone disulfonate/bromide system in contrast to $81 kW^{-1}h^{-1} for vanadium systems.[78] In terms of the utilized separator, perfluorinated proton exchange membranes have the highest costs, followed by ion-exchange membranes, and finally porous separators having the lowest costs. Thus, the application of polymer-based organic charge-storage materials is attractive.[34] In addition, it was found that flow batteries using electrolytes based on organic solvents are far from being cost-competitive.[75] Hence, water in combination with sodium chloride as the supporting electrolyte is the recommended electrolyte, both from a cost and also a safety point of view.

The common flow-battery systems (VRFB, Fe/Cr, and Zn/Br$_2$) illustrate evident concerns regarding the environmental or social impact in the case of the production of the primary materials, damage, or disposal. For example, ore mining may be executed in developing countries with unsatisfactory social and environmental standards (e.g. zinc mining in China) or the utilized electrolytes may reveal significant hazards.[23,34,79]

Furthermore, the overall efficiency of flow batteries is reduced by the control systems as well as the permanently

operating pumps, which circulate the electrolytes between the electrochemical cell and the storage tanks. An active temperature management, which is necessary in VRFBs, can have an additional effect on the overall efficiency.[62]

The significant challenge for organic charge-storage materials is the long-term stability of the electrolyte. In contrast to metals, which form stable ions, organic compounds tend to undergo side reactions when they are either oxidized or reduced; in particular, if radical ions are formed. Reactions with the electrolyte can also be observed. For example, the widely used redox-active cathode material TEMPO undergoes disproportionation reactions at pH values lower 2.5 and the oxoammonium cation is not stable in basic media. Thus, a long lifecycle of the active materials can only be reached under optimized conditions.

Electrolytes based on metal redox-active materials can be galvanically recycled. Thermal recycling seems to be the best option for electrolytes based on organic active materials.

3. History: "The Metal Age"

A brief summary of flow batteries based on metal redox-active materials is presented in this section; a much more detailed overview is given, for example, by Yu and co-workers,[80] Soloveichik,[81] Skyllas-Kazackos et al.,[82] and Noack et al.[83]

The first battery type similar to todays flow batteries was patented by Kangro in 1949.[84] This system employed $Cr_2(SO_4)_3$ as the cathode and anode active material and 2 M sulfuric acid as the supporting electrolyte, and yielded a cell voltage of 1.75 V.[85] $TiCl_4$, Ti/Fe, Ti/Cr, Ti/Cl_2, and Cr/Fe were also proposed as redox-active materials.[84–86] The National Aeronautics and Space Administration (NASA) reported an Fe/Cr system in the 1970s, which gained much attention.[87] The employed redox couples were $Fe^{3+}/Fe^{2+}//Cr^{3+}/Cr^{2+}$ solvated in an acidified electrolyte. A 1 kW/13 kWh demonstrator was fabricated that worked in combination with a photovoltaic array. Unfortunately, this RFB system suffered from fast capacity decay caused by crossover of the redox-active species across the utilized anion-exchange membrane. As a consequence of this, mixed electrolytes were utilized in following studies. At that time, no satisfactory membrane was commercially available and custom-made membranes could not meet the requirements in terms of resistivity and selectivity. A decade later Skyllas-Kazacos and Robins patented the VRFB.[88] This system utilizes the redox couples $VO_2^+/VO^{2+}//V^{3+}/V^{2+}$, and an open circuit voltage (OCV) of 1.3 V was reached.[89] The origin of the aqueous Zn/Br_2 battery goes back to a patent of Bradley from 1885.[90] The first hybrid-flow batteries were developed by Exxon and Gould Inc. in the 1970s and 1980s, respectively.[91,92] $ZnBr_2$ is employed as the redox-active material. During the charging process, $Zn^{2+}_{(aq)}$ is reduced to $Zn^0_{(s)}$ and a deposit is formed on the electrode (electroplating). At the counter electrode, Br^- is oxidized to elemental bromine. Complexing agents, for example, quaternary ammonium salts are added to reduce the hazard of liquid or gaseous bromine.[93,94] The Fe/Cr, Zn/Br$_2$, all-vanadium, Fe/Zn, and all-iron flow batteries are either

already commercially available or under development by several companies. A wide range of other metal-based redox-active materials were investigated on a laboratory scale over the last few years. For example, Zn/Ce,[59,95] Zn/Ni,[29] Ru,[96,97] UO_2^+/U^{3+},[98] Mn^{3+}/Mn^{2+},[99] all-Cu,[100] Pb/PbO$_2$,[101] Ti/Fe,[102] Cu/PbO$_2$,[103] and Li[104–106] were all investigated. Besides these metal-based systems, the metal-free H/Br flow battery also represents a promising system.[30,81,83,107,108]

3.1. Current Trends in Metal RFBs

Despite the fact that the systems described previously were already proposed several decades ago, they are still the subject of current research. A lot of interesting technologies have been reported over the last few months. Li et al. increased the energy density of VRFBs by utilizing a mixed HCl and H_2SO_4 supporting electrolyte, and increased the solubility of vanadium to 2.5 M (energy density ca. 40 Wh L^{-1}).[109] The group of Skyllas-Kazacos reported a high energy density VRFB.[70] Typical concentrations of the redox-active vanadium were in the range of 1.6 and 2 M in commercial systems. Supersaturated solutions were obtained by the addition of inorganic additives; 1 wt% H_3PO_4 and 2 wt% $(NH_4)_2SO_4$ were added to obtain 3 M vanadium solutions. This system is a significant advancement and increases the theoretical capacity to 80 Ah L^{-1}. However, a material utilization of only 62% was reached in charge/discharge experiments, thus leading to an achievable capacity of 49.6 Ah L^{-1}.[70]

An ambipolar Zn/polyiodide HFB with a superior energy density of 167 Wh L^{-1} was reported by Wang and co-workers.[110] The authors utilized a 5 M ZnI_2 solution both as the catholyte and anolyte. Publications on the iron/chromium RFBs have decreased significantly in recent years. Nevertheless, the EnerVault Corporation installed a 250 kW/ 1 MWh facility in California, USA, in summer 2015.

Lithium-flow batteries represent an emerging topic in the scientific community that tries to combine the benefits of Li-ion batteries and flow batteries. The main benefit is an elevated cell potential in the range of 2.5 to 3 V, which is possible because of the utilization of an organic solvent. Chen et al. reported a non-aqueous sulfur-impregnated carbon composite dispersion as the catholyte and combined it with a Li$_{(s)}$ anode.[111] This setup leads to an average discharging voltage of 2 V and an immense volumetric capacity of 294 Ah L^{-1}.

A similar design was reported by Mubeen et al.[112] Here, the concept of a carbon particle based cathode was extended by the utilization of a carbon particle based anode, where Zn^{2+}/Zn^0 was the anode active material. Several cathode active materials were investigated: Cu, MnO, Br, and again S.

Huang et al. reported a lithium iodide HFB with a potential energy density of 670 Wh L^{-1}. However, only a flow battery with an energy density of about 0.4 Wh L^{-1} has so far been realized.[113]

Metal-air flow batteries are of great interest, as they promise high energy and low-cost battery systems. A lithium-air battery was reported, in which an ionic liquid was used.[114]

The vanadium-air redox-flow battery (VARFB) or vanadium-oxygen fuel cell (VOFC) increases the energy density significantly compared to VRFBs.[115–119] The common anodic redox-reaction of V^{3+}/V^{2+} is utilized in combination with an oxygen cathode.

Wei et al. reported an aqueous, pH-neutral Fe/S flow battery.[120] This battery features 1M solutions of Na_2S_2 and $K_3Fe(CN)_6$ as the catholyte and anolyte, respectively, which leads to a capacity of 11.7 AhL^{-1}. A drawback of this battery system is the limited cell voltage of 0.91 V. However, this system represents a notable innovation regarding the acquisition costs compared to VRFBs, which are stated to be only one third of those of vanadium in terms of raw material cost per kWh.

Manohar et al. presented an $FeCl_2$ hybrid-flow battery with an improved efficiency. This system employed the redox couples $Fe^{3+}/Fe^{2+}//Fe^{2+}/Fe^0$ with a standard redox-cell potential of 1.2 V. Hydrogen evolution is problematic in iron chloride batteries and drastically reduces the efficiency of the battery. The authors suppressed this process by utilizing ascorbic acid and $InCl_3$ as additives as well as an increased pH value of 2.[121]

Gong et al. reported a Zn/Fe HFB with system capital costs of 100 $\$kW^{-1}h^{-1}$.[74] The system features a volumetric capacity of 12 AhL^{-1} and utilizes $FeCl_2$ and $Na_2[Zn(OH)_4]$ as the catholyte and anolyte, respectively.

Some of these systems show several problems in relation to the environmental and sociopolitical impact, or the system design is too complicated for large-scale batteries. The compatibility of flow batteries with these considerations can be improved by the utilization of regenerative and non-corrosive electrolytes. As a consequence, the implementation of organic redox-active species is a first move in this direction. Moreover, the utilization of organic materials can reduce the acquisition costs per kWh compared to cost-intensive metals. The utilization of organic redox-active materials in flow-battery applications will be discussed in detail in the following section.

4. Rise of the Organic Active Materials

As already mentioned, conventional metal-based flow batteries have several drawbacks, which limit their commercial success. However, the development of RFBs based on inexpensive and sustainable redox-active organic materials can overcome these drawbacks.

When we use the term "organic" or "all-organic" in association with flow batteries, we refer only to the redox-active materials utilized and not to the solvent or the supporting electrolyte, which can be water or any organic solvent capable of dissolving the organic redox-active material.

Intensive research on the use of RFBs as flexible and scalable energy-storage systems came to the conclusion that future RFB systems, irrespective of their use for domestic or large-scale application, have to utilize noncorrosive, safe, and especially low-cost charge-storage materials.[34, 122, 123] In the last decade the first steps were taken by the utilization of

organic additives such as complexing agents,[124, 125] followed by metal-ligand complexes with organic ligands as charge-storage materials,[58, 96] and subsequently to flow batteries with an inorganic and an organic active material.[32, 126] In recent years, organic/halogen,[78, 127] and all-organic RFBs were developed.[128, 129] Organic compounds offer the potential to overcome several metal-related problems and may lead to sophisticated high-performing RFBs for tomorrow's electricity grids. For that purpose, new organic redox-active charge-storage materials have to be discovered and investigated for application in RFBs. These materials can be low-molar-mass compounds (molar mass $< 1000\ gmol^{-1}$ and ≤ 2 repeating redox-active units) or redox-active polymers, both with well-defined electrochemical properties. Selected examples are summarized in Figure 4.
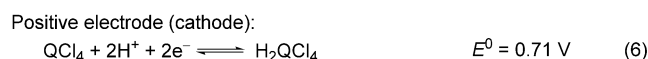
4.1. Flow Batteries with Organic/Inorganic Redox-Active Materials

These RFBs utilize one redox-active organic material and a second inorganic species for the charge-storage process. This classification refers only to the active material employed. Other components, such as solvents, metal-based supporting electrolytes, and additives of any kind, are excluded.

4.1.1. Flow Batteries with Low-Molar-Mass Organic/Inorganic Redox-Active Materials
4.1.1.1. Quinone-Based Redox-Active Materials

The first organic/inorganic flow battery was developed by Xu et al. in 2009.[131] The single-flow cadmium/chloranil flow battery utilized Cd^0 as the anode-active material and an acidic $CdSO_4$ solution as the anolyte. The insoluble tetrachloro-*p*-benzoquinone (chloranil, QCl_4) was utilized as the organic cathode.

Positive electrode (cathode):
$$QCl_4 + 2H^+ + 2e^- \rightleftharpoons H_2QCl_4 \qquad E^0 = 0.71\ V \qquad (6)$$

Negative electrode (anode):
$$Cd \rightleftharpoons Cd^{2+} + 2e^- \qquad E^0 = -0.40\ V \qquad (7)$$

The authors fabricated a small test cell consisting of a QCl_4/carbon black cathode, a copper foil as the current collector, and an aqueous electrolyte consisting of 0.5 M $CdSO_4$, 1 M $(NH_4)_2SO_4$, and 0.5 M H_2SO_4. The insolubility of QCl_4, H_2QCl_4, and Cd^0 meant that the single-flow battery could be operated without utilization of a membrane. The fabricated battery revealed an average charge voltage of 1.18 V and an average discharge voltage of 0.97 V at a current density of 10 $mAcm^{-2}$. The coulombic efficiency reached 99% with an energy efficiency of 82% over the first 100 charge/discharge cycles.

The reported single-flow battery has the advantage of being membrane-free and, therefore, saving investment costs. The requirement of a strongly acidic electrolyte for the chloranil cathode, however, can be seen as a drawback.
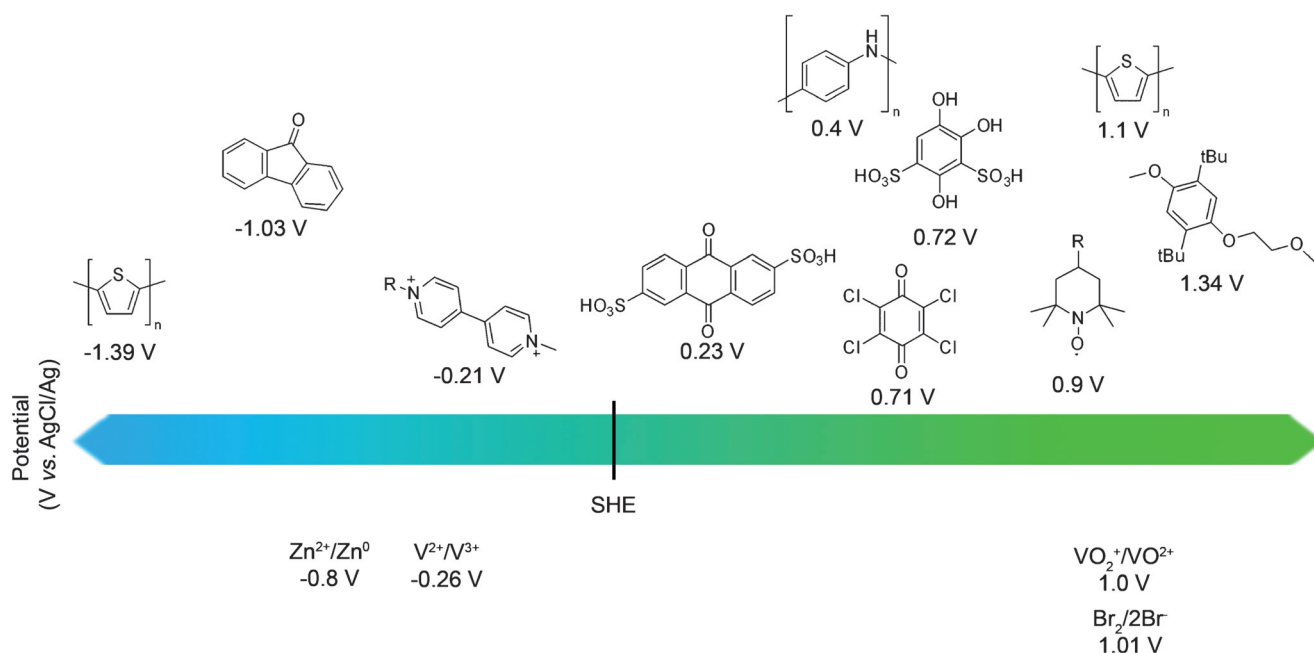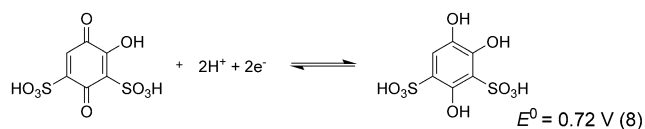
Figure 4. Schematic overview of selected organic/inorganic active materials and their redox potentials; recalculated to a SHE reference if measured against another reference electrode. Conversion factors: SHE to AgCl/Ag = +0.197 V, SHE to SCE = +0.241 V, SHE to Fc⁺/Fc = +0.750 V;[130] SHE: standard hydrogen electrode, SCE: standard calomel electrode, Fc: ferrocene.[35, 41, 78, 126, 131–137]

In a subsequent study, the authors reported a lead/4,5-dibenzoquinone-1,3-benzenedisulfonate (tiron) HFB.[133] The test cell, equipped with a Nafion 115 membrane, utilized 0.25 M tiron in 3 M H_2SO_4 as the cathode material and a Pb^{2+}/Pb^0 hybrid anode.

Positive electrode (cathode):

$$E^0 = 0.72 \text{ V} \quad (8)$$

Negative electrode (anode):

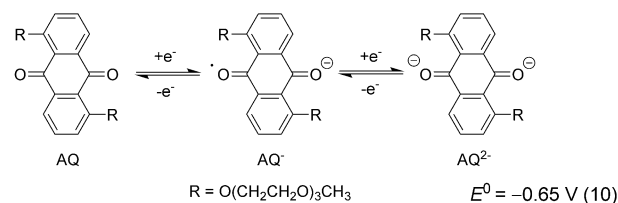$$Pb + SO_4^{2-} \rightleftharpoons PbSO_4 + 2e^- \qquad E^0 = -0.35 \text{ V} \quad (9)$$

The charge/discharge test indicated an irreversible reaction at an elevated cell voltage and a low coulombic efficiency of 38% in the first cycle. An average coulombic efficiency of 93% and an average energy efficiency of 82% were achieved over the following nine cycles. The cycling of the battery was performed at 10 mA cm⁻² and the energy density was calculated to be 2.8 Wh L⁻¹. Similar to chloranil, the electrochemical behavior of tiron is strongly pH-dependent and the reported HFB can only be operated with electrolytes below pH 4. Furthermore, tiron exhibited an electrochemical hydroxylation during the first electrolysis, which causes a part of the active material to undergo an irreversible side reaction.

In 2012, Wang et al. reported an organic/inorganic HFB based on an anthraquinone derivative with methoxytriethyleneglycol substituents (15D3GAQ) dissolved in propylene carbonate as the organic cathode material, lithium as the anode, and $LiPF_6$ as the supporting electrolyte.[138]

Anthraquinone derivatives are well-known as organic cathode materials for lithium-ion batteries and, therefore, the redox mechanism has been extensively investigated.[139–143] The ethylene glycol moieties promote solubility, in particular in non-aqueous polar solvents, and a concentration of 0.25 M has been reached.

Positive electrode (cathode):

R = O(CH₂CH₂O)₃CH₃

$$E^0 = -0.65 \text{ V} \quad (10)$$

Negative electrode (anode):

$$Li \rightleftharpoons Li^+ + 1e^- \qquad E^0 = -3.04 \text{ V}^{[144]} \quad (11)$$

The electrochemical performance of 15D3GAQ was investigated in a static test cell, equipped with a porous polypropylene separator and 0.25 M 15D3GAQ and 1 M $LiPF_6$ in propylene carbonate as the supporting electrolyte and anode-active material, respectively. The static cell was charged and discharged in the range of 1.8 and 2.8 V, and demonstrated an energy efficiency of 82% and a theoretical specific discharge energy density of 25 Wh L⁻¹ over nine cycles. A current density of 0.1 mA cm⁻² was applied in the first cycle, but was raised progressively up to 10 mA cm⁻².[138] Nevertheless, an optimization of the electrolyte is necessary to overcome an observed decline in the discharge capacity, caused by side reactions between anthraquinone and the carbonate-based solvents.

As a consequence of the considerable potential of anthraquinones as organic redox-active materials, Bachman et al. investigated the redox chemistry, the influence of substituents on the redox potential, and the solvation free energy of about 50 anthraquinone derivatives by density functional theory (DFT) calculations.[145] The study revealed that a complete methylation of the anthraquinone core decreases the reduction potential by 0.47 V and that the introduction of oxymethyldioxolane substituents (with a similar reduction window and adequate oxidative stability) enhances the solvation energy.[145]

In a preliminary study, Quan et al. used conducting cyclic voltammetry measurements to investigate the electrochemical properties of anthraquinone in buffered and unbufferd aqueous solution at different pH values.[146] In these studies, quinoidic structures revealed promising properties for charge-storage applications in flow batteries. The solubility could be ensured by the choice of suitable substituents, and the redox potential can be adjusted in the same manner.

In 2015, Lin et al. reported an alkaline quinone flow battery by utilizing commercially available 2,6-dihydroxyanthraquin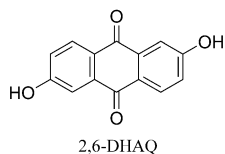one (2,6-DHAQ, Figure 5) and ferrocyanide/ferricyanide.[147] This system represents an improvement over the organic/halogen aqueous RFB (Huskinson et al.;[78] a detailed description can be found in Section 4.2). The ferrocyanide/ferricyanide replaced the dangerous $Br_2/2\,Br^-$ redox couple. In contrast to this, ferrocyanide/ferricyanide has a low toxicity and is nonvolatile. The authors claimed on the basis of these characteristics that the reported RFB can be used as a cost-efficient, nontoxic, nonflammable, and safe energy-storage system. However, the strongly alkaline electrolyte is also highly corrosive (pH 14; 1 M KOH).

Figure 5. Schematic representation of the chemical structure of 2,6-dihydroxyanthraquinone (2,6-DHAQ).

The introduced electron-donating hydroxy groups in the 2,6-DHAQ reduce the reduction potential and increase the battery voltage.[78,147] Furthermore, the hydroxy groups are deprotonated in alkaline solution, which improves the solubility up to 0.6 M in a 1 M KOH solution at room temperature. The reduction potential is independent of the pH value above pH 12. Hence, the reversibility of the redox reaction was investigated by cyclic voltammetry at pH 14, and displayed a rapid kinetic rate constant and two one-electron reductions separated by 60 mV.

The electrochemical performance was investigated in a flow cell containing a Nafion 212 membrane, 0.5 M 2,6-DHAQ dipotassium salt in 1 M KOH solution as the anolyte, and 0.4 M $K_4Fe(CN)_6$ in 1 M KOH solution as the catholyte; this performance correlates to an energy density of 6.8 $Wh\,L^{-1}$. A constant current density of 100 $mA\,cm^{-2}$ was applied, and 100 charge/discharge cycles with a current efficiency above 99% and a steady energy efficiency of 84% were measured (Figure 6).[147]
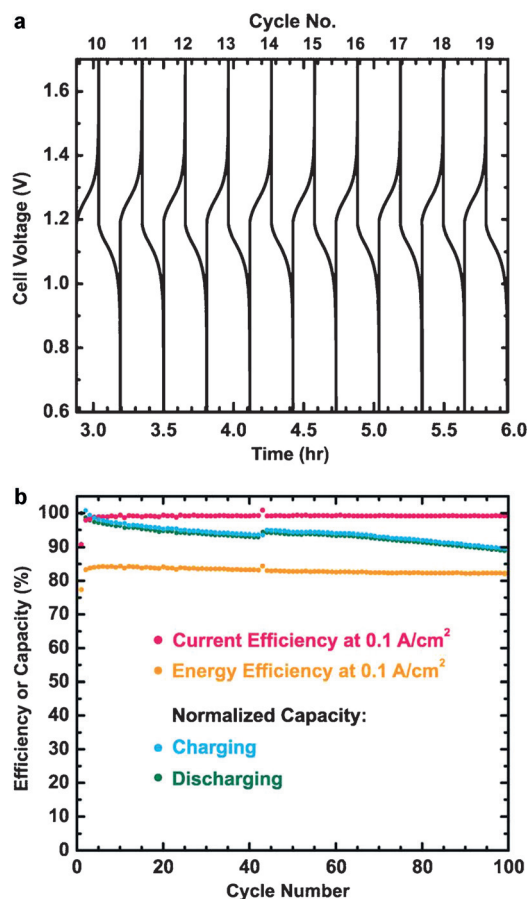

Figure 6. Cell cycling performance of the alkaline quinone flow battery. a) Representative voltage versus time curves during 100 charge/discharge cycles at 0.1 $A\,cm^{-2}$, recorded between the 10th and 19th cycles. b) Capacity retention, current efficiency, and energy efficiency values of 100 cycles. Normalized capacity is evaluated on the basis of the capacity of the first charge and discharge cycle.[147]
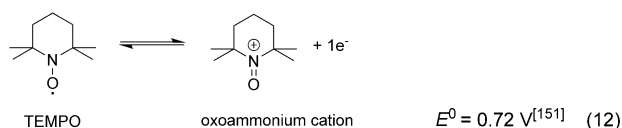
4.1.1.2. TEMPO-Based Redox-Active Materials

Wei et al. reported in 2014 a lithium HFB containing 2,2,6,6-tetramethylpiperidine-1-oxyl (TEMPO) as the organic active material.[126] TEMPO is a stable, heterocyclic nitroxide radical that had already been explored as a redox-active material for semiorganic lithium and all-organic radical batteries.[148–150]

Cyclic voltammetry studies of TEMPO with $LiPF_6$ as the conductive salt, dissolved in ethylene carbonate (EC)/propylene carbonate (PC)/ethyl methyl carbonate (EMC; weight ratio of 4:1:5), demonstrated highly reversible redox reactions and a one-electron transfer for the nitroxide radical/oxoammonium cation redox couple [Eq. (12)].

To investigate the electrochemical performance of TEMPO in a flow-battery environment, a non-aqueous hybrid Li/TEMPO flow cell with a hybrid anode of lithium foil and graphite felt, a polyethylene-based porous separator, and graphite felt as the cathode was fabricated. Furthermore, a fluoroethylene carbonate (FEC) additive was added to protect the Li anode. TEMPO, dissolved in a mixture of EC/PC/EMC (weight ratio of 4:1:5), as well as $LiPF_6$ as support-

Positive electrode (cathode):

TEMPO ⇌ oxoammonium cation + 1e⁻

$E^0 = 0.72\ V$ [151]   (12)

Negative electrode (anode):

Li ⇌ Li⁺ + 1e⁻

$E^0 = -3.04\ V$ [144]   (13)

ing electrolyte and anode active material, was added to both cell compartments, but only circulated on the cathode side.

Battery tests with various concentrations of TEMPO (0.1 M, 0.8 M, 1.5 M, and 2.0 M) were performed. One hundred consecutive charge/discharge cycles were demonstrated at a TEMPO concentration of 0.1 M in 1.0 M $LiPF_6$ EC/PC/EMC with 15 wt% FEC additive at a current density of 5 mA cm⁻². Thereby, an energy efficiency of 86%, a coulombic efficiency of 99%, a voltage efficiency of 87%, and an average capacity retention of 99.8% per cycle were achieved. At the same current density, but with 0.8 M TEMPO in 1.2 M $LiPF_6$ with 15 wt% FEC additive, the performance in terms of the stability was reduced and a theoretical energy density of 64 Wh L⁻¹ during the first 30 cycles was achieved.[126]

The obtained results, in particular for higher concentrations up to 2.0 M TEMPO, with a theoretical energy density of 126 Wh L⁻¹ surpass the performance of other conventional aqueous and non-aqueous RFBs.[129,152–154] These high energy densities are facilitated by the large difference in the redox potentials, which lead to a system voltage of 3.5 V.[126]

The authors reported a high solubility of TEMPO up to 5.2 M in the solvent mixture, which offers the possibility to further increase the energy density.[126] However, the viscosity of the electrolyte also rises as the concentration increases, and results in a high power demand of the pumps for circulating the electrolytes. Thus, the overall system efficiency of a practical RFB is significantly lowered. Furthermore, such high energy densities at a limited maximal current density are not practical in the everyday use of a flow battery, since the cell stack would need to be prohibitively large.

Takechi et al. discussed that a concentration higher than 2.0 M is difficult to obtain for redox-active organic materials in aqueous and non-aqueous solvents, and came to the conclusion that the use of an ionic liquid could overcome this limitation and enable higher maximal theoretical energy densities.[41] The TEMPO derivative 4-methoxy-2,2,6,6-tetramethylpiperidine-1-oxyl [MeO-TEMPO, redox mechanism in Eq. (12)] was selected as the organic redox-active compound and lithium bis(trifluoromethanesulfonyl)imide (LiTFSI) as the supporting electrolyte. The TFSI anion exhibits an uncommon plasticizing effect and induces the formation of a supercooled liquid.

A mixture of MeO-TEMPO and LiTFSI (MTLT) in a molar ratio of 1:1 features a "self-melting behavior and formed a smooth viscous liquid".[41] MTLT (1:1) showed the best energy density, but also had a significant viscosity (η) above 10 Pa s at room temperature, which is caused by the concentration of the redox-active material, and is 500 times higher than the viscosity of classical electrolytes applied in

VRFBs.[155,156] The viscosity was reduced by the addition of water to the molten MTLT (1:1), thereby enabling application in RFBs. MTLT (1:1) plus 17 wt% H_2O exhibited a viscosity of 72 mPa s and a conductivity (σ) of 3.1 mS cm⁻¹. However, the capacity was lowered to 1.11 mAh.

The system was chosen as the catholyte for further investigations in flow-cell tests. A hybrid battery with a lithium ion conducting glass ceramic (LIC-GC) membrane and lithium metal as the anode was constructed. MTLT (1:1) plus 17 wt% of H_2O was utilized as the catholyte and 1 M LiTFSI in propylene carbonate as the anolyte. A non-pumped battery showed over 20 charge/discharge cycles at a current density of 0.1 mA cm⁻² with a charge/discharge capacity of 93% and 92%, a coulombic efficiency of 99%, a capacity retention of 84%, a calculated energy density of 200 Wh L⁻¹, and a specific energy of 155 Wh kg⁻¹, which are the highest energy densities achieved for organic/inorganic flow batteries to date. The charge/discharge tests in a flow battery revealed a steady capacity retention with a broad range of flow rates at restricted current densities from 0.1 to 1 mA cm⁻².[41] In particular, this limited current rating, which is induced by the LIC-GC separator and the carbonate-based organic anolyte, prevents commercialization of this system.

4.1.1.3. *Alkoxybenzene-Based Redox-Active Materials*

Huang et al. reported redox-active low-molar-mass compounds as cathode materials for non-aqueous RFBs in 2014.[134] Based on the general structure of dimethoxy-di-*tert*-butylbenzene (Figure 7), which is responsible for the electrochemical properties and stability, oligoethylene oxide chains were introduced to increase the moderate solubility (ca. 0.4 M) in carbonate-based polar solvents and, consequently, the energy density.

Besides the better solubility, the authors also observed an alteration of the physical properties at room temperature, from a solid state (DBBB) over a semi-liquid (ANL-10) to liquid (ANL-8, ANL-9). This enables new possibilities to significantly increase the energy density. The utilization of a supporting electrolyte, which is soluble in the charge-storage material, would allow the solvent to be replaced.

The three charge-storage materials (ANL-8, ANL-9, and ANL-10) were investigated by cyclic voltammetry in propylene carbonate with 0.2 M $LiBF_4$ and exhibited a good electro-
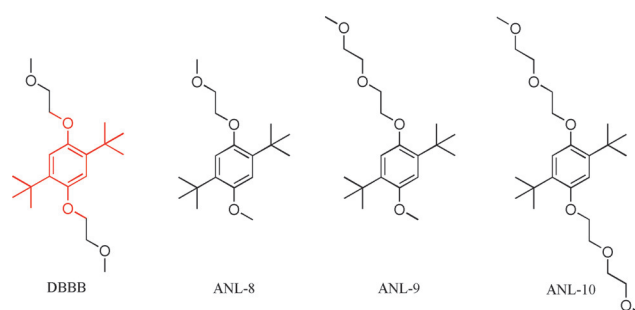

Figure 7. Chemical structures of 2,5-di-*tert*-butyl-1,4-bis(2-methoxyethoxy)benzene (DBBB) and modified derivatives ANL-8, ANL-9, and ANL-10.

chemical reversibility and redox potentials of around 4.0 V versus Li+/Li. However, ANL-8 features a diffusion coefficient of the same order of magnitude as vanadium,[157,158] DBBB,[159,160] and several quinone derivatives.[78,161] The battery tests were performed with 1 mM ANL-8 plus 0.5 M LiBF₄ as a conducting salt, dissolved in propylene carbonate, at a constant charging current of 0.4 mA in a bulk-electrolysis cell, where an energy density of 0.05 WhL⁻¹ for the catholyte could be achieved. The obtained voltage, energy efficiency, and capacity profiles revealed a deviant behavior at the first cycle, which indicates a side reaction during the first charging process. The energy efficiency of the first cycle was only 37%, whereas the value for the following cycles was 81%.[134]

Huang et al. also investigated several other 1,4-dimethoxybenzene derivatives as redox-active materials for non-aqueous RFBs in a subsequent study.[162] Starting from 2,5-di-*tert*-butyl-1,4-bis(2-methoxyethoxy)benzene) (DBBB), well-known as a material for protection against overcharging in lithium-ion batteries,[163] the authors modified the sterically demanding substituent groups to increase the solubility. Five substituted 1,4-dimethoxybenzene derivatives were generated and further investigated. Cyclic voltammetry measurements showed that 2,3-dimethyl-1,4-dimethoxybenzene (23DDB) and 2,5-dimethyl-1,4-dimethoxybenzene (25DDB, Figure 8) underwent quasireversible redox reactions and a one-electron transfer.
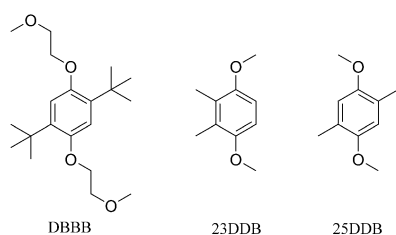

Figure 8. Chemical structures of 2,5-di-*tert*-butyl-1,4-bis(2-methoxyethoxy)benzene (DBBB), 2,3-dimethyl-1,4-dimethoxybenzene (23DDB), and 2,5-dimethyl-1,4-dimethoxybenzene (25DBB).

Thus, 23DDB and 25DBB were further explored through galvanostatical cycling in a bulk electrolysis cell. The utilized electrolytes contained 1 mM redox-active material and 0.5 M LiTFSI dissolved in polycarbonate. The corresponding electrolytes were charged/discharged from 0 to 50% state of charge (SOC) over 100 cycles at a charging current of 0.4 mA.

The calculated energy density of 0.05 WhL⁻¹ for the cathode material as well as the charge and discharge capacities illustrate the drawbacks of these two derivatives. These studies showed that 50% of 25DBB and 50% of 23DBB turned irreversibly into a non-rechargeable species after approximately 48 cycles and 15 cycles, respectively. Accordingly, the average coulombic efficiency of 25DDB is about 90% for the first 40 cycles and of 23DBB between 75 and 80% for the first 20 cycles.[162] In contrast to the good electrochemical properties of these alkoxybenzenes seen from CV measurements, the battery tests revealed several concerns regarding the chemical reversibility of the active

material. Therefore, their general suitability as active materials is questionable.

In contrast, TEMPO-containing organic/inorganic flow batteries showed elevated energy densities (64 to 200 WhL⁻¹, for the cathode materials), which was facilitated by the utilization of a Li(s) anode and an electrolyte based on an organic carbonate. However, the current rating was restricted and safety concerns remain. In contrast, the quinone battery has excellent current ratings, but a limited energy density. However, the safety aspect is improved.
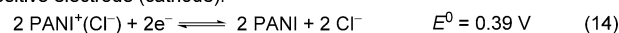
On the basis of these results, anthraquinone and TEMPO derivatives are the most promising organic charge-storage materials because of their interesting redox potentials, good chemical reversibility, and fast kinetics. However, future challenges concern the development of suitable substituents to further improve the performance and the solubility of these redox-active units for RFB applications.

4.1.2. *Flow Batteries with Polymer-Based Organic/Inorganic Redox-Active Materials*

A significant drawback of common RFBs is the often utilized and expensive Nafion ion-exchange membrane. The application of polymers with sufficiently high molar masses and linear, starlike, hyperbranched, or cyclic architectures instead of low-molar-mass compounds as organic redox-active materials allow the use of cost-efficient size-exclusion/dialysis membranes and microporous separators.[32–36]

In 2013, Zhao et al. reported the first polymer-based HFB, which utilized polyaniline (PANI) particles as the charge-storage material. The authors constructed a HFB based on a zinc plate as the anode, a cost-efficient polypropylene microporous separator, and a flowing PANI microparticle suspension in ZnCl₂ and NH₄Cl as the catholyte.[35]

Positive electrode (cathode):

$$2\,PANI^+(Cl^-) + 2e^- \rightleftharpoons 2\,PANI + 2\,Cl^- \qquad E^0 = 0.39\ V \qquad (14)$$

Negative electrode (anode):

$$Zn \rightleftharpoons Zn^{2+} + 2e^- \qquad E^0 = -0.76\ V^{[164]} \qquad (15)$$

The fabricated flow battery was operated for 32 charge/discharge cycles. Current densities in the range of 10 to 30 mA cm⁻² were applied, whereby a linear decrease in the achieved capacity with increasing current densities was observed. Coulombic efficiencies of 97% and a decrease in the discharge capacity retention of 0.07% per cycle were obtained. Furthermore, the calculated maximal theoretical energy density of 66.5 WhL⁻¹ exceeds the value of about 25 WhL⁻¹ of conventional VRFBs.[35,109] However, the charge/discharge cycling at a current density of 20 mA cm⁻² with an average discharge voltage of 1.1 V and a discharge capacity density of 115.2 mAh g⁻¹ (150 g L⁻¹ PANI suspension) reaches a maximal energy density of 9.5 WhL⁻¹. Furthermore, coulombic efficiencies of over 100% were achieved in some experiments. The authors ascribed this phenomenon to the oxidation of the PANI particles by

atmospheric oxygen. In the discharging procedure, these chemically oxidized particles can be reduced by consumption of the supporting electrolyte $Zn^{2+}_{(aq)}$. Hence, a long-term decline in the battery performance is apparent. In addition, the application of a conductive polymer as the charge-storage material is not favored, as the redox potential of the polymer changes with the degree of oxidation (level of charging). This leads to steep potential curves in a battery application. The redox system was improved in a following study by using Ag-doped PANI particles.[165]

Nagarjuna et al. presented a poly(vinylbenzylethylviologen) nonconductive polymer as the cathode material for non-aqueous flow batteries in 2014.[36] The authors synthesized five vinylbenzylethylviologen polymers with molar masses (M_n) of 21, 104, 158, 233, and 318 kg mol^{-1}. These redox-active polymers (RAPs) featured a good solubility (above 2.1 M per repeating unit) in non-aqueous solvents such as acetonitrile or propylene carbonate, as well as chemically reversible redox reactions in cyclic voltammetry measurements. The authors employed a Celgard microporous trilayer PE/PP separator and observed, at cell-operating conditions, a polymer crossover of 7% for the RAP with a molar mass of 318 kg mol^{-1} over a period of 6 h.

The electrochemical performance was investigated by using a non-aqueous redox-flow-cell configuration, which contained a metal oxide auxiliary electrode. The utilized flow-cell setup was not completely charged/discharged and demonstrated a charge capacity of 44% and a coulombic efficiency of above 45% at a C rate of 1/10.

In the same year, Sukegawa et al. described a 2,2,6,6-tetramethylpiperidin-1-oxyl (TEMPO) substituted bottle-brush polymer with a well-defined size as a potential catholyte for flow-battery applications.[166] Bottlebrush polymers feature a lower viscosity than linear polymers with the same molar mass. Furthermore, the structure of a bottlebrush polymer is spatially tunable, for example, by the ratio of the length of the side chain and the main chain. The authors synthesized the target polymer poly(norbornene)-*g*-poly(4-methacryloyloxy-2,2,6,6-tetramethylpiperidine-1-oxyl) (PNB-*g*-PTMA) by a "grafting-through" technique.

The fabricated half-cell included a single flow channel, an AgCl/Ag reference electrode, and a carbon mesh current collector as the working electrode. 0.1 M PNB-*g*-PTMA ($M_n = 2.2 \times 10^5$ g mol^{-1}) plus 0.1 M *n*-tetrabutylammonium perchlorate as a supporting electrolyte dissolved in ethylene carbonate/diethyl carbonate (1:1 in volume) were constantly circulated through the system. A half-cell charge/discharge experiment revealed a plateau potential at 1.0 V versus AgCl/Ag and a charge capacity utilization of 95% at a C-rate of 1. Furthermore, 1% of the utilized polymer passed through the porous separator over a period of 24 h.

The reported PNB-*g*-PTMA bottlebrush polymer is a notable innovation in the field of polymer-based RFBs (pRFB) and is designed, in particular, to counteract the increased viscosity of the electrolyte, one of the greatest challenges pRFBs have to overcome. However, the solubility has to be further increased to improve the energy density of this system. Similar concepts should be applied to water-soluble polymers.

In 2016, Winsberg et al. reported a novel, "green" poly-(TEMPO)/zinc semiorganic HFB.[32,33] The authors combined the benefits of the zinc/halogen flow battery with those of an all-organic polymer RFB,[34] which uses low-cost organic polymers as redox-active materials as well as a simple size-exclusion membrane as separator. Compared to recently reported zinc-halogen HFBs, this battery shows significant improvements in terms of corrosion and environmental impact. Three TEMPO-containing polymers were applied, one P(TMA-*co*-METAC) and two P(TMA-*co*-PEGMA)s (TMA = TEMPO methacrylate, METAC = [2-(methacryloyloxy)ethyl]trimethylammonium chloride, PEGMA = poly-(ethylene glycol) methacrylate) with various monomer to co-monomer ratios, as redox-active materials in carbonate-based and aqueous electrolyte systems. A hybrid flow battery was constructed with a dialysis membrane as the separator, zinc foil as the anode, and P(TMA-*co*-PEGMA) as the cathode active material. The supporting electrolyte and anolyte used was $Zn(ClO_4)_2 \times 6H_2O$ in ethylene carbonate (EC)/dimethyl carbonate (DMC)/diethyl carbonate (DEC; v:v:v, 1:1:1). A stable charge/discharge cycling was performed over 500 cycles and revealed an average capacity decay of 0.04% per cycle and coulombic efficiencies of >99.7%. Current densities in the range of 0.5 to 4 mA cm^{-2} were applied. Here, a linear decrease in the energy efficiency with increasing current density was observed. The authors demonstrated a maximum capacity of 6.1 Ah L^{-1}.

Battery tests in aqueous electrolyte systems were performed to reach higher applicable current densities. The utilized aqueous catholyte contained P(TEMPO-*co*-METAC) as the cathode active material plus 0.71 M NaCl, 0.08 M ZnCl$_2$, and 0.08 M NH$_4$Cl as the supporting electrolyte. Current densities up to 12 mA cm^{-2} and an energy density of 1.9 Wh L^{-1} were reached. Additionally, the coulombic efficiency with a maximum of 99% at 12 mA cm^{-2} always remained above 90% and the energy efficiency always above 80%. A good long-term stability with 1000 consecutive charge/discharge cycles, with an initial discharge capacity retention of 79%, were achieved (Figure 9).

Current densities up to 20 mA cm^{-2} and an energy density of 4.1 Wh L^{-1} were achieved with an aqueous catholyte containing P(TEMPO-*co*-PEGMA) plus 1.0 M ZnCl$_2$ and 1.0 M NH$_4$Cl as the supporting electrolyte. A material activity of 88% was reached, and the coulombic efficiency stayed mostly above 90% at various current densities. However, a linear decrease in the capacity occurred at increasing current densities.

This organic/inorganic HFB permits a stable potential window of up to 2 V (OCV 1.7 V) in an aqueous electrolyte system. Furthermore, contamination with oxygen is unproblematic and an expensive process to render the HFB inert is unnecessary.

In a following study the authors demonstrated the application of core-corona micelles with a TEMPO-containing corona as the cathode active material.[33] The application of a micellar catholyte reduced the viscosity compared to the previously reported linear TEMPO-containing polymers. Again, a stable battery cycling was demonstrated over 1000 consecutive charge/discharge cycles with 95% retention of
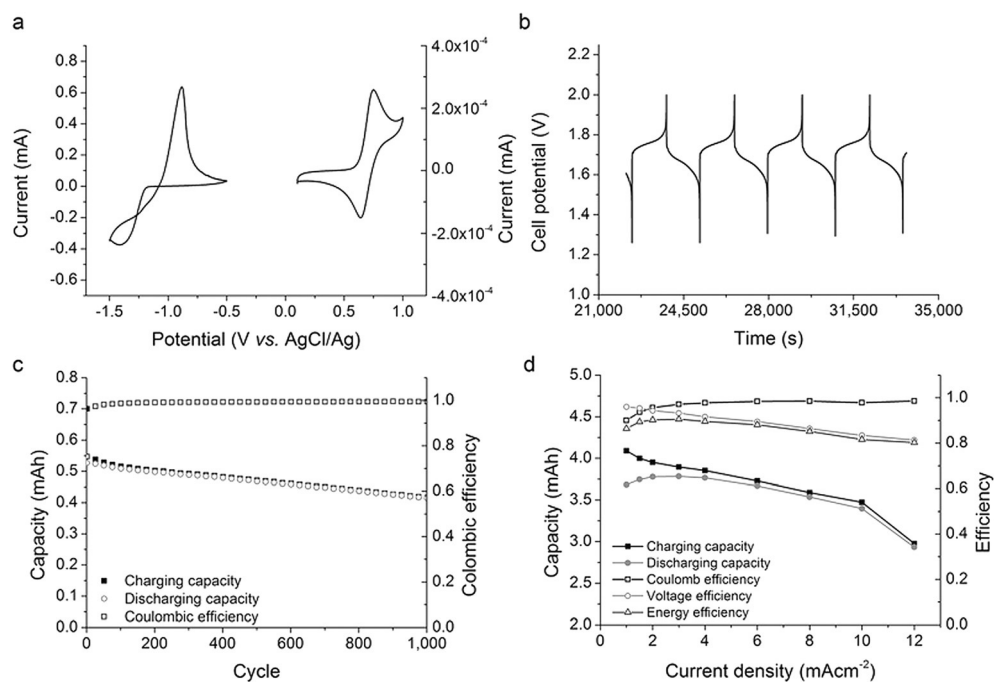
Figure 9. a) Cyclic voltammogram of an aqueous solution of 0.1 M zinc chloride and 0.01 M poly(TEMPO). Scan rate: 50 mV s^{-1}. b) Exemplary charging/discharging curves at a current density of 2 mA cm^{-2}, aqueous catholyte; polymer solution in NaCl, ZnCl$_2$, NH$_4$Cl with a capacity of 1.1 Ah L^{-1}, flow rate: 20 mL min^{-1}. c) Long-term stability test, cycling of a static cell. d) Electrical performance: capacity, coulombic, voltage, and energy efficiency depending on the applied current density.[32]

cell setup contained a Nafion 212 proton-exchange membrane, 3 M HBr and 0.5 M Br$_2$ as the catholyte, and 1 M AQDS in 1 M H$_2$SO$_4$ as the anolyte.

The charge/discharge experiment, conducted at 40 °C, revealed a stable performance over 20 cycles, a discharge capacity retention of 99 %, and a current efficiency of around 99 % at a current density of 500 mA cm^{-2}. The applied electrolyte had a calculated energy density of 9.4 Wh L^{-1}. These results, which are comparable with those of the quinone-based organic/inorganic flow battery,[147] illustrate that anthraquinones represent a promising organic anode material for RFB applications. Their synthesis from inexpensive starting materials is straightforward and

initial discharge capacity and applicable current densities in the range of 0.2 to 5 mA cm^{-2}. The battery featured an energy density of 0.8 Wh L^{-1}.

From these described polymer-based organic/inorganic flow batteries, the combination of zinc/organic polymer[32,33,35] shows the greatest potential for further developments. As mentioned before, TEMPO-based redox-active materials,[32,33,166] in particular, are promising charge-storage materials because of their well-defined redox behavior. The good long-term stability is ensured by the hindered recombination of two TEMPO moieties because of steric effects, the delocalization of the radical electron, and an unfavored NO−ON bond formation.

In contrast to RFBs based on low-molar-mass organic charge-storage materials, polymer-based RFBs allow the utilization of cost-efficient size-exclusion (dialysis) membranes and microporous separators. Nevertheless, potential challenges such as an increased synthesis effort, solubility, and viscosity properties have to be addressed in future studies.

4.2. Redox-Flow Batteries Based on Organic/Halogen Redox-Active Materials

These RFB systems operate without the utilization of any metal as the redox-active material. The first was reported by Huskinson et al. in 2014.[78] It is based on 9,10-anthraquinone-2,7-disulfonic acid (AQDS) in H$_2$SO$_4$ as the anolyte and Br$_2$/2 Br$^-$ in HBr as the catholyte (Figure 10). The employed flow-

Positive electrode (cathode):

$$2\,Br^- \rightleftharpoons Br_2 + 2e^- \qquad\qquad E^0 = 1.07\,V^{[167]} \quad (16)$$

Negative electrode (anode):

$$AQDS + 2e^- + 2H^+ \rightleftharpoons H_2AQDS \qquad\qquad E^0 = 0.22\,V \quad (17)$$

can be easily scaled up. Furthermore, AQDS undergoes a very fast and chemically reversible two-electron two-proton reduction in sulfuric acid. A kinetic rate constant (k_0) of 7.2 × 10^{-3} cm s^{-1} was measured, which is very high compared to the corresponding values of other metal-based redox-active materials used in flow-battery applications.[23] The utilized AQDS has a solubility of greater than 1 M at pH 0, which can be increased by the introduction of functional groups, such as hydroxy groups. Nevertheless, the described quinone/hydroquinone redox couple also shows some drawbacks, such as limited solubility in aqueous media. Furthermore, the necessity to conduct the battery tests at a temperature of 40 °C increases the energy demand and lowers the over-all efficiency of the system.

In a following study, the authors described in detail the cycling performance of this flow battery.[168] The initially applied Nafion 212 membrane was replaced by a Nafion 115 membrane and the electrolyte contained 1 M AQDS in 1 M H$_2$SO$_4$ as the anolyte (100 mL) as well as 3 M HBr and 0.5 M Br$_2$ as the catholyte (120 mL). At a current density of 250 mA cm^{-2}, the flow cell exhibited an average discharge capacity retention of nearly 100 % per cycle over 106 cycles.
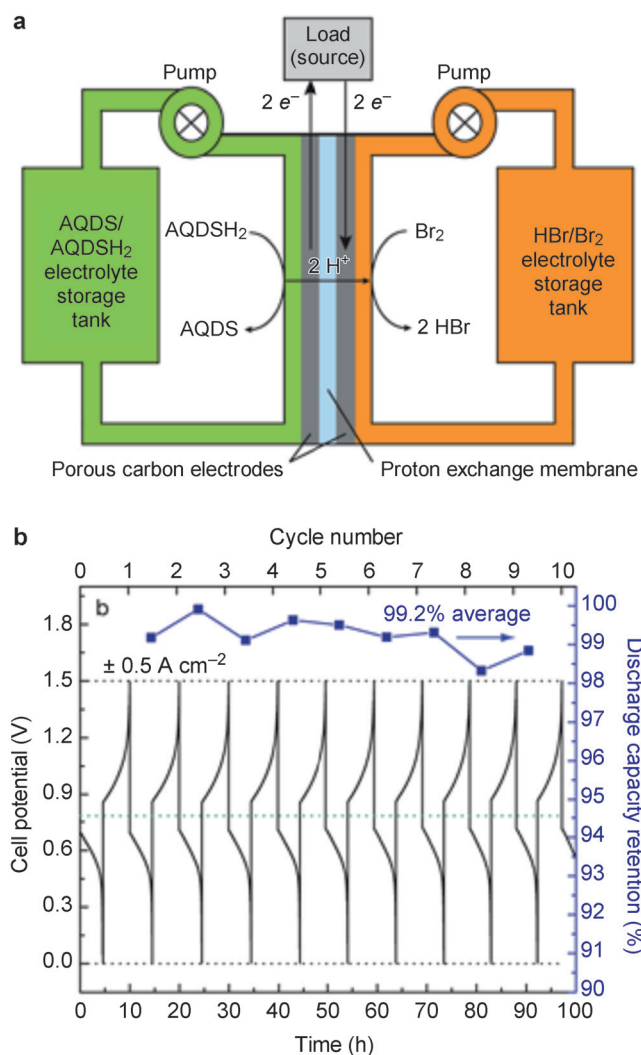
Figure 10. a) Schematic diagram of a cell. The discharge mode is shown; the arrows are reversed for the electrolysis/charge mode. AQDSH$_2$ refers to the reduced form of AQDS. b) Constant-current cycling at 0.5 A cm^{-2} at 40°C using a 3 M HBr, 0.5 M Br$_2$ solution on the positive side and a 1 M AQDS, 1 M H$_2$SO$_4$ solution on the negative side; the discharge capacity retention is indicated for each cycle.[78]

At a current density of 750 mA cm^{-2}, the flow cell was cycled 750 times and revealed an average current efficiency of 98% as well as an average discharge capacity retention of nearly 100% per cycle.

In 2015, Chen et al. also reported a quinone/bromide RFB based on the cell design developed by Huskinson et al.[127] In contrast to the earlier study,[78] baked (400°C in air for 24 h) SGL carbon paper (ca. 400 μm thick) was utilized instead of pretreated Toray carbon paper (7.5 μm thick, uncompressed) as electrodes to enhance the power output. The cell operated at 40°C using AQDS in 1 M H$_2$SO$_4$ as the anolyte and 3 M HBr together with 2 M Br$_2$ as the catholyte. Although the anolyte and the anode compartments were not altered, the composition of the catholyte was modified. The redox potential and, thus, the cell voltage could be increased by reducing the concentration of HBr or enhancing the Br$_2$ concentration.

Adversely, a decrease in the HBr concentration led to an increase in the membrane and electrolyte resistance and additionally to a high rate of bromine crossover. The described flow cell revealed a short-circuit current density above 4000 mA cm^{-2} at 90% SOC and a peak galvanic power density of 1 Wcm^{-2}.[127] These data represent a significant improvement in reference to the published results of Huskinson et al.[78] Furthermore, the achieved peak galvanic power density of 1.0 Wcm^{-2} is 75% higher than the maximum values of previously published VRFBs.[169]

In a subsequent study, Chen et al. also reported a cycling analysis of the quinone/bromide RFB.[170] The authors used 1 M AQDS in 1 M H$_2$SO$_4$ as the anolyte (25 mL) and 3.5 M HBr in combination with 0.5 M Br$_2$ as the catholyte. The battery tests were performed at 30°C, with current densities in the range of 100 to 1000 mA cm^{-2} with the aim of investigating the impact of the current density on the voltage polarization, charge capacity, as well as, current, voltage, and energy efficiency. Since the focus was on the organic redox-active anode material, a significant excess of the active species on the cathode side was employed, which led to a ratio of positive to negative charge capacity of 5:36. The authors observed linear polarization curves at current densities up to 250 mA cm^{-2} at a SOC in the range of 10 to 90%. The overvoltage increased as the current density increased, and resulted in an earlier accomplished voltage limit, which led to a decrease in the utilized charge/discharge capacity. Leakage of the anolyte, destruction of the redox-active anode material, and the Br$_2$ crossover also resulted in a decrease in the charge/discharge capacity. Thus, 40% of the theoretical capacity was achievable at a current density of 1000 mA cm^{-2}. On the basis of the obtained results, Chen et al. were able to explain the relationship between current density and coulombic, voltage, and energy efficiency through established equations.

Zhang et al. reported in 2016 an improvement to Li's[171] investigated 3D numerical model and simulation study of the quinone/bromide RFB.[172] A 3D non-isothermal transient model with added graphite plates as well as a temperature field was utilized to investigate the influence of current, temperature, and electrolyte flow rate on the battery performance of the quinone/bromide RFB. The flow-cell setup was designed in accordance with that of Huskinson et al.[78] Battery tests were simulated with current densities in the range of 50 to 400 mA cm^{-2} with the aim of investigating the impact of the current density on the battery performance. Furthermore, battery tests were performed with a current density of 200 mA cm^{-2} and 500 mA cm^{-2} to compare the obtained computational results with experimental data; a good comparability was found. The investigated 3D model showed a strong influence of the flow channel structure and temperatures > 30°C on the battery performance.

As mentioned before, anthraquinone derivatives revealed excellent properties as charge-storage materials in battery applications. However, the solubility needs to be increased to 2 M and bromine needs to be replaced by a safer organic cathode active material in future studies.

4.3. Redox-Flow Batteries with Organic Redox-Active Materials for the Catholyte and Anolyte

As previously discussed, the focus of research in the field of flow batteries should be the development of a RFB using noncorrosive, safe, and in particular low-cost redox-active organic charge-storage materials.[34] Thereby, promising redox-active low-molar-mass compounds as well as redox-active polymers are of interest. Both systems have inherent advantages; small molecules have the advantages of little or no synthetic effort, potential high solubilities, and good diffusion coefficients, whereas polymers offer the prospect of using more cost-efficient and robust separators compared to ion-selective membranes.

The development of a so-called all-organic equivalent to a VRFB with a bipolar redox-active material is of high interest, because this material would be able to undergo oxidation as well as reduction reactions and could, therefore, be applied as both the cathode- and anode-active material. This feature would reduce the synthesis effort of the whole process and potentially overcome the problem of cross-contamination, since a slow mixing of the electrolytes would only lead to a reduced coulombic efficiency but not to a continuously decreasing charge/discharge capacity.[28]

4.3.1. Redox-Flow Batteries with Low-Molar-Mass Organic Redox-Active Materials

4.3.1.1. Symmetric Redox-Flow Batteries with Bipolar Organic Redox-Active Materials

In 2011, Rasmussen investigated pyrazine-based cyano-azacarbon derivatives as potential bipolar organic redox-active materials.[173] Cyclic voltammetry measurements of the derivative 9,10-butyl-2,3,6,7-tetracyano-1,4,5,8,9,10-hexaanthracene revealed a chemical reversibility for the oxidation as well as the reduction reaction, and a possible cell potential of nearly 3 V.

A few years later, Potash et al. reported a symmetric redox-flow battery, which utilizes diaminoanthraquinones (DAAQs) as bipolar redox-active materials.[28] Several commercially available DAAQs were investigated by cyclic voltammetry, with the DAAQ derivative Disperse Blue 134 (DB-134) showing a good reversibility in both the oxidation and reduction reactions. Therefore, this material was further investigated in a glass H-cell, where the compartments were separated by a glass frit with medium porosity. Solutions with a concentration of 50 mM DB-134 and 100 mM tetrabutylammoniumperchlorate in acetonitrile/toluene (v/v; 3:2) were charged/discharged at a current of 2 mA. The authors demonstrated three charge/discharge cycles with a subsequent reversal of polarization. Depending on the cycling method, a coulombic efficiency in the range of 85 and 61 %, a voltage efficiency between 53 and 45 %, and an energy efficiency in the range of 43 and 28 % were achieved. The continuous decrease can be explained by a slow degradation of the redox-active DB-134. The observed energy density was 0.94 WhL^{-1}.[28] These moderate results of the battery tests are induced by the limited solubility of the utilized DB-134 in

the electrolyte, the observed crossover through the porous glass frit, and the incomplete inert battery setup.

In 2016, Duan et al. published an alternative approach to a non-aqueous symmetric redox-flow battery by using the commercially available 2-phenyl-4,4,5,5-tetramethylimidazoline-1-oxyl oxide (PTIO, Figure 11), a nitronyl nitroxide radical, as the bipolar organic redox-active material.[174]
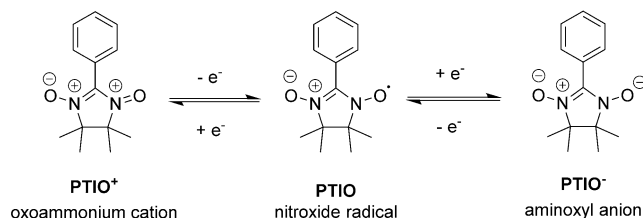

Figure 11. Electrochemical reactions of PTIO.

Compounds containing nitronyl nitroxides were first described in 1968 by Osiecki et al., and subsequently investigated electrochemically in detail and used in several magnetic applications.[175–183]

PTIO, as a novel charge-storage material for RFBs, features a potential high solubility of about 2.6 M in acetonitrile. However, a flow cell with a PTIO concentration > 0.5 M has not been realized so far. Furthermore, a crossover of the redox-active material through the separator, which limits the CE, and a high viscosity of the electrolyte was observed. The state of charge and the concentration of PTIO was monitored by FTIR spectroscopy. The cycling performance of a flow cell that utilized a Daramic porous separator and 0.5 M PTIO with 1 M $TBAPF_6$/acetonitrile as the supporting electrolyte was investigated. The test cell completed over 15 cycles at a current density of 20 mA cm^{-2} at a coulombic efficiency of about 90 %, a voltage efficiency of 67 %, an energy efficiency of 60 %, and an energy density of 9 WhL^{-1} during charge as well as 5 WhL^{-1} during discharge. These results are far better than the values of the symmetric redox-flow battery reported by Potash et al.[28]

However, independent of the utilized PTIO concentration, the demonstrated flow cells show a continuous capacity loss, probably because of an electrolyte imbalance and/or chemical instability of the charged redox-active material.

4.3.1.2. Asymmetric Redox-Flow Batteries with Organic Redox-Active Materials in Organic Electrolytes

In 2011, Li et al. reported the first RFB with two redox-active organic compounds, TEMPO and *N*-methylphthalimide, as the cathode and anode active material.[129]

Cyclic voltammetry measurements showed quasireversible redox reactions for both compounds with a voltage of approximately 1.6 V. The authors performed battery tests with a test cell containing a Nepem 117 cation-exchange membrane by using 0.1 M TEMPO and 0.1 M *N*-methylphthalimide, both dissolved in anhydrous acetonitrile plus 1 M $NaClO_4$ supporting electrolyte, as the catholyte and anolyte, respectively. The static test cell was operated at a current

Positive electrode (cathode):

$E^0 = 0.72$ V[151]   (18)

Negative electrode (anode):

$E^0 = -0.88$ V   (19)
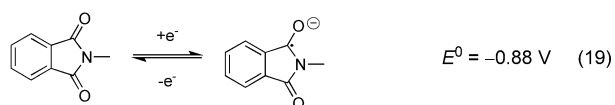
density of 0.35 mA cm^{-2}. The coulombic efficiency exceeded 90% and an energy density of 1.7 Wh L^{-1} was achieved during the first 20 charge/discharge cycles.

The increased voltage of 1.6 V in comparison to VRFBs represents a significant advantage and illustrates the flexibility of all-organic RFBs. However, the capacity and current rating of this system are restricted by the organic electrolyte.

In 2012, Brushett et al. reported a non-aqueous RFB by using 2,5-di-*tert*-butyl-1,4-bis(2-methoxyethoxy)benzene (DBBB) and 2,3,6-trimethylquinoxaline (TMeQ) as redox-active materials.[159] The fundamental electrochemical properties of these compounds were investigated by cyclic voltammetry and revealed a high redox reversibility at around 4 V versus Li$^+$/Li for DBBB and two reversible redox reactions at 2.48 and 2.8 V versus Li$^+$/Li for the TMeQ. The authors developed a "proof-of-concept coin-cell flow battery" to verify the feasibility of these redox-active molecules for application in a RFB. This setup, normally appropriate for lithium-ion/thin-film battery tests, contained a Nafion 117 membrane with 0.05 M DBBB and 0.05 M TMeQ in 0.2 M LiBF$_4$ dissolved in propylene carbonate as the catholyte and anolyte, respectively. As a consequence of the unoptimized cell design and the limited solubility of DBBB, the maximum observed capacity of this coin-cell test device was 0.6 Ah L^{-1} at a current density of 0.0625 mA cm^{-2}.[159] This is much lower than the high capacity of common VRFBs.[70] A battery cycling was performed over 30 cycles, and coulombic efficiencies of around 70% and energy efficiencies of around 37% were achieved.[159]

The alkoxybenzenes DBBB and the previously discussed ANL-8,[134] 23DBB, and 25DB,[162] all showed rather poor results in regard to solubility and chemical reversibility. As a result, their utilization in flow batteries is not reasonable and future research should focus on different active materials.

Despite this limited performance, Su and co-workers also investigated DBBB as a redox-active cathode material for non-aqueous RFBs.[160] Based on the results from Brushett et al.,[159] the authors developed an automated electrolyte preparation as well as a characterization platform, which allowed combinatorial screening of a large number of electrolytes, including the redox-active DBBB, several alkali ion salts as supporting electrolytes, and organic carbonates as solvents. The highest solubility (>0.5 M) and also ionic conductivity (>5 mS cm^{-1}) were achieved for a solvent mixture of linear and cyclic carbonates with lithium hexafluorophosphate (LiPF$_6$) as supporting electrolyte and bis(trifluoromethane)sulfonamide lithium (LiTFSI) as an additive.[160] However, the ionic conductivity is significantly higher in

aqueous solution than in organic solvents. For example, the TEMPO/methylviologen system in aqueous solution exhibits an ionic conductivity of about 100 mS cm^{-1}.[135] Thus, aqueous organic RFBs seem to be a better alternative to the non-aqueous organic systems.

Kaur et al. reported in 2015 the phenothiazine derivative 3,7-bis(trifluoromethyl)-*N*-ethylphenothiazine (BCF3EPT) as an organic cathode material and 2,3,6-trimethylquinoxaline (TMeQ) as an anode material.

Positive electrode (cathode):

$E^0 = 0.86$ V   (20)

Negative electrode (anode):


$E^0 = -0.54$ & -0.24 V   (21)
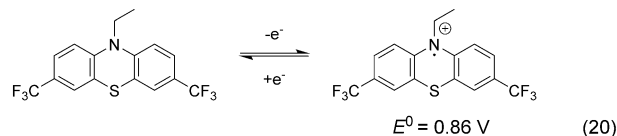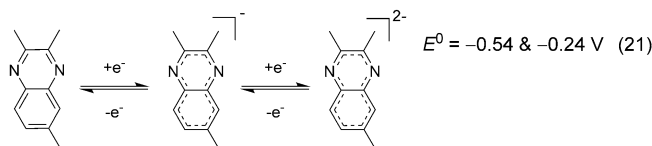
The cell performance was investigated by using a static Swagelok cell, in combination with a Nafion 117 membrane and 0.2 M LiBF$_4$ in propylene carbonate as the supporting electrolyte. The static Swagelok cell with 0.05 M BCF3EPT/TMeQ showed a coulombic efficiency of approximately 92% and an energy density of around 0.84 Wh L^{-1}. The battery cycling experiment revealed that this flow cell lost nearly all of its capacity after 100 consecutive charge/discharge cycles. A second battery with an increased capacity (0.15 M of each redox-active species) demonstrated a stable performance over 60 cycles. Thereby, an average charge/discharge capacity of 0.44 and 0.37 mAh g^{-1}, a coulombic efficiency of almost 89%, and an energy density of approximate 2.5 Wh L^{-1} were achieved. However, a battery with an increased concentration of 0.35 M showed a rapidly decreasing charge/discharge capacity that decreased to zero after 20 cycles.[184]

The current system exhibits some serious drawbacks such as the restricted solubility of the TMeQ anolyte and the non-optimized membrane selection, which results in a crossover of the organic compounds. Furthermore, it was observed that the utilized BCF3EPT catholyte undergoes a second irreversible oxidation in the charging procedure, which leads to a decrease in the overall capacity. Additionally, an adverse side reaction of the anode active material cannot be excluded, thereby rendering this material, up to now, questionable for RFB applications.

Wei et al. reported another non-aqueous RFB with ANL-8 and 9-fluorenone (FL) as the cathode and anode material, respectively.[136] These two small molecules demonstrated good solubility, or in the case of ANL-8 (which is liquid at room temperature) good miscibility with several organic solvents, and well-defined electrochemical properties. To investigate the performance of the ANL-8/FL battery, a test cell was fabricated with a Daramic microporous

Positive electrode (cathode):

$E^0 = 1.34$ V (22)

Negative electrode (anode):


$E^0 = -0.9$ V (23)
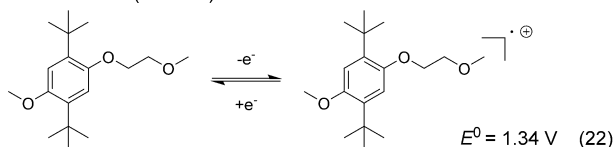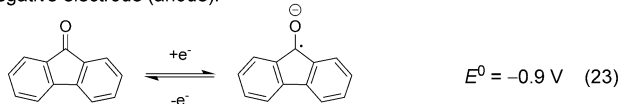
polyethylene/silica separator, 0.5 M FL, and 0.5 M ANL-8 in acetonitrile with 1.0 M tetraethylammonium bis(trifluoromethylsulfonyl)imide as the conducting salt. Over 100 charge/discharge cycles, at a current density of 15 mA cm^{-2}, the flow cell demonstrated a cell voltage of > 2 V, coulombic efficiencies of 86 %, a voltage efficiency of 83 %, and an energy efficiency of 71 %. The theoretical energy density was 15 Wh L^{-1}, of which 73 % could be utilized.

The achieved performance parameters are much higher than those for the reported system by Brushett et al.[159] and Li et al.[129] Despite this, a demonstration of a stable charge/discharge capacity retention over a few cycles was not possible and a constant decrease over 100 cycles starting from 5.8 to 1.2 Ah L^{-1} was observed, which represents a loss of nearly 80 %. Similar to the previously discussed studies with ANL-8 and DBBB, the unsuitability of alkoxybenzenes is affirmed.

4.3.1.3. Asymmetric Redox-Flow Batteries with Organic Redox-Active Materials in Aqueous Electrolytes

In 2014, Yang et al. reported the first aqueous all-organic RFB. They used a water-soluble 1,2-benzoquinone-3,5-disulfonic acid (BQDS) as the organic cathode active material and anthraquinone-2-sulfonic acid (AQS) as well as anthraquinone-2,6-disulfonic acid as the organic anode active material.[128]

Positive electrode (cathode):

$E^0 = 0.85$ V[128] (24)

+ 2e$^-$ + 2H$^+$

Negative electrode (anode):


$E^0 = 0.09$ V (25)

+ 2e$^-$ + 2H$^+$
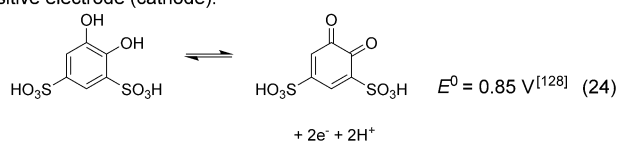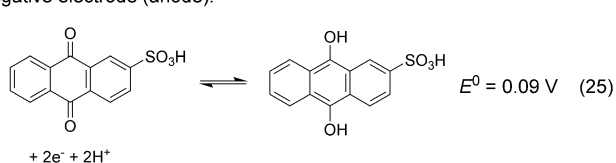
The authors developed a redox-flow cell with a membrane electrode assembly, which was fabricated from coated carbon

paper electrodes and a Nafion 117 membrane. The flow cell contained 0.2 M BQDS and 0.2 M AQS in 1 M H$_2$SO$_4$ as the catholyte and anolyte, respectively. The electrolytes had a calculated energy density of 1.25 Wh L^{-1}. A charge/discharge experiment was conducted over 12 cycles at a current density of 10 mA cm^{-2}, whereby a capacity retention of 90 % was reached.[128] Limiting factors of these organic charge-storage materials are their moderate solubility in aqueous media and the observed mass transport of the reactants. These factors and the non-optimized battery setup lead to a restriction of the possible current density. The reported system can be seen as an improvement compared to the AQDS/bromide RFB in terms of safety, as the toxic bromine catholyte is replaced by BQDS. However, the capacity and the electrical performance are significantly inferior.

Zhang et al. reported an aqueous RFB with the already known water-soluble 1,2-benzoquinone-3,5-disulfonic acid (BQDS) as the catholyte and an inexpensive anthraquinone derivative, 3,4-dihydroxy-9,10-anthraquinone-2-sulfonic acid (ARS), as the anolyte.[128,161]

Positive electrode (cathode):

$E^0 = 0.91$ V[161] (26)

+ 2e$^-$ + 2H$^+$

Negative electrode (anode):


$E^0 = 0.08$ V (27)

+ 2e$^-$ + 2H$^+$
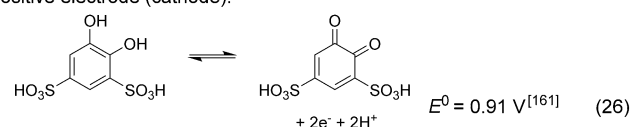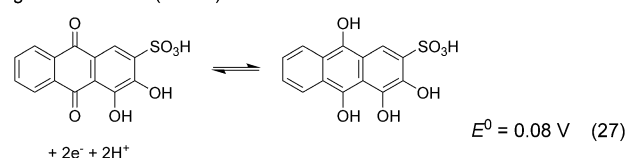
Both charge-storage materials are commercially available. Electrochemical investigations showed that ARS exhibits a two-electron redox process and that the redox reactions of both molecules are highly reversible. The utilized laboratory flow cell comprised copper plates as current collectors and a Nafion 212 proton-exchange membrane. Charge/discharge measurements with 0.05 M BQDS and 0.05 M ARS in 1 M H$_2$SO$_4$ as the catholyte and anolyte, respectively, were performed with various current densities of 20, 30, and 60 mA cm^{-2} to investigate the cell performance. Three charge/discharge cycles with an average discharge capacity of 90 mA h^{-1}, a calculated discharge capacity retention of around 98 %, as well as a columbic efficiency of 99 % were achieved. The maximal power density of 10.6 mW cm^{-2} was accomplished at 80 % SOC at a current density of 60 mA cm^{-2}.[161]

The authors obtained good columbic efficiencies through fast charging and slow discharging cycling, but the unoptimized flow-cell setup led to a voltage loss. Furthermore, the observed energy density of 0.4 Wh L^{-1} and the current density is limited by the restricted solubility of the utilized redox-active molecules, especially of the ARS.

At the end of 2015, Liu et al. described an aqueous RFB with 4-hydroxy-2,2,6,6-tetramethylpiperidine-1-oxyl (4-HO-TEMPO) and methylviologen (MV) as the organic redox-active catholyte and anolyte, respectively. The authors applied the derivative 4-HO-TEMPO instead of common TEMPO as the cathode active material because of its higher water solubility of up to 2.1M.[135] However, the solubility of 4-HO-TEMPO in NaCl solution is only approximately 0.5 M.

Positive electrode (cathode):
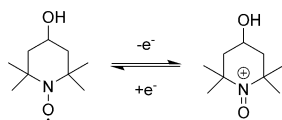
$$E^0 = 0.80 \text{ V} \quad (28)$$

Negative electrode (anode):
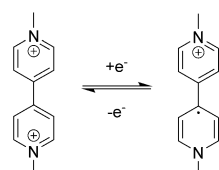
$$E^0 = -0.45 \text{ V} \quad (29)$$

NaCl was utilized as the supporting electrolyte and an anion-exchange membrane allowed selective transport of chloride ions. CV and RDE measurements showed that MV and 4-HO-TEMPO displayed chemically reversible and diffusion-controlled redox reactions. Battery tests were performed at room temperature at concentrations of 0.1M and 0.5M of the redox-active material in aqueous 1.0M or 1.5M solution of NaCl at current densities in the range of 20 to 100 mAcm^{-2}. 72% of the theoretical capacity at a current density of 60 mAcm^{-2} was utilized. A voltage efficiency of 62%, an energy efficiency of 63%, and a coulombic efficiency above 99% were achieved over 100 charge/discharge cycles. The theoretic energy density of this system was 8.4 WhL^{-1} (Figure 12).[135]

The reported flow battery exhibited a moderate energy density and good coulombic efficiencies. However, the voltage efficiency and, thus, the energy efficiency strongly limit the performance of this system. One of the benefits is the low price and commercial availability of the employed active materials. The major problem, which affects the long-term usability of this system, is the side reaction of the 4-HO-TEMPO. The oxoammonium cation [which is generated in the charging procedure; Eq. (28)] is capable of oxidizing alcohols, thereby leading to a self-oxidation of 4-HO-TEMPO to 4-keto-TEMP-hydroxylamine.[185]

The development of RFBs with inexpensive and sustainable organic redox-active materials as well as low-cost membranes may overcome the existing drawbacks of inorganic RFBs, such as the VRFB. In particular, a symmetric RFB with an organic bipolar redox-active material could represent an organic alternative to state-of-the-art VRFBs. Nevertheless, research in this field is in its infancy and needs further intensive investigations on potential organic bipolar redox-active materials. A bipolar material that can be utilized in the electrochemical window of water is of particular
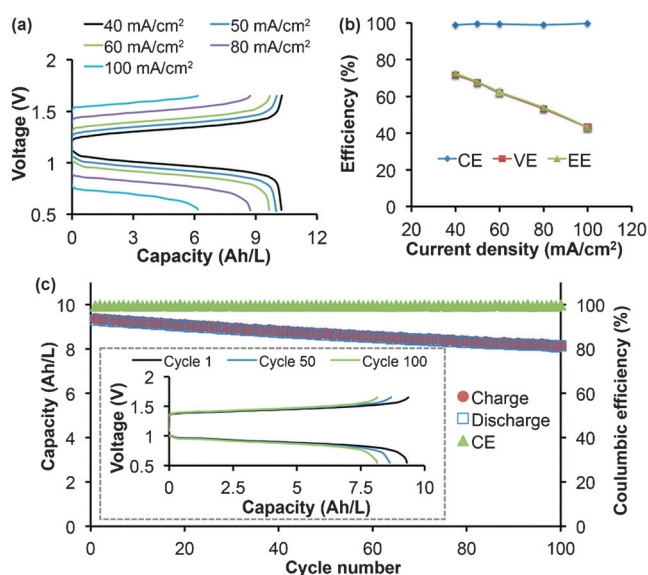

Figure 12. a) Representative charge and discharge profiles of the MV/4-HO-TEMPO RFB (0.5 M) at cycling rates from 20 to 100 mAcm^{-2}. b) Plots of Coulombic efficiency, voltage efficiency, and energy efficiency versus current density of the cell. c) Capacity and coulombic efficiency versus cycling numbers of the cell at 60 mAcm^{-2}. Conditions: anolyte, 0.5 M MV in 1.5 M NaCl aqueous solution; catholyte, 0.5 M 4-HO-TEMPO in 1.5 M NaCl aqueous solution; flow rate, 20 mLmin^{-1}.[135]

interest. Asymmetric RFBs are also an interesting topic for further developments so as to increase the capacity and, thus, the energy density. The choice of the right charge-storage materials and highly selective membranes already allows good long-term capacity retentions and low crossover reactions to be achieved.

4.3.2. Redox-Flow Batteries with Polymer-Based Organic Active Materials

The first polymer-based non-aqueous symmetric RFB was reported by Oh et al. in 2014. The authors fabricated an electrolyte based on a suspension of polythiophene (PT) particles, where PT serves as the bipolar redox-active material.[132] A high stability of the redox reactions and pronounced n-doping and p-doping was exhibited. The observed electrochemical redox processes at −2.0 and 0.5 V versus Ag$^+$/Ag enabled a high cell potential of 2.5 V. The performance of these bipolar redox-active conductive particles was investigated in a flow-cell setup with an anion-exchange membrane and carbon black as the conductive additive. Polythiophene microparticles (8.41 gL^{-1}) were dispersed in a solution of 1M tetraethylammonium tetrafluoroborate (TEABF$_4$) in propylene carbonate. At a current density of 0.5 mAcm^{-2}, the flow battery demonstrated a stable charge/discharge behavior over 20 cycles with a high energy efficiency of 61% and a maximal observed energy density of 2.7 WhL^{-1}.[132] Besides the advantage that the conjugated polymer particles lead to a decrease in the electric resistance inside the cell, the application of conjugated polymer particles led to some major drawbacks, such as

steep potential curves and the possibility of clogged flow channels as a result of agglomerated particles.

Water offers several advantages over organic electrolyte solvents: It is nonflammable, inexpensive, and allows for high ion mobility, for example, low ohmic resistance. For this reason, Janoschka et al. evaluated numerous water-soluble polymers (polymethacrylates and polystyrenes) for application in an aqueous RFB.[186] A special focus was on their rheological, thermal, and electrochemical properties with a target of < 20 mPa s to ensure the efficient operation of a pumped RFB. A novel battery type to replace common ion-exchange membranes and highly corrosive, acidic electrolyte solutions with inexpensive dialysis membranes and pH-neutral sodium chloride solutions was reported by using optimized polymers, which employ TEMPO and viologen as the redox-active moieties (Figure 13).[34, 186]

The dialysis membrane showed a good retention of the redox-active materials and a low resistance of $1.14 \, \Omega \, cm^2$, which is in the range of Nafion. The high ion mobility in water led to current densities of up to 100 mA cm^{-2} being attained. The long-term stability of the system was demonstrated in a static test cell by repeated charging/discharging over 10 000 cycles with 80 % capacity retention. Furthermore, a pumped flow cell with an increased volumetric capacity of 10 Ah L^{-1} demonstrated a capacity retention of around 80 % after 95 consecutive charge/discharge cycles. The faster fade in capacity can be explained by a side reaction, possibly induced by oxygen. Although this novel system may lay the foundation for a new RFB working principle (polymer plus dialysis membrane), capacity limitations of currently 10 Wh L^{-1} still need to be overcome, for example, by substituting linear for hyperbranched polymers.

Winsberg et al. reported a poly(boron dipyrromethene)-based flow battery.[187] Boron dipyrromethenes (BODIPYs) are frequently used as chemosensors and laser dyes. Besides their special optical properties, several BODIPYs feature chemically reversible oxidation and reduction reactions, which render them a potential bipolar redox-active material for flow-battery applications and, thus, an organic alternative to VRFBs (Figure 14).
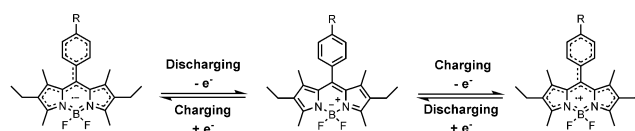

Figure 14. Redox mechanism of the utilized BODIPY derivative.

The authors synthesized styrene-based polymers with pendant BODIPY moieties and fabricated an organic solution-based battery by using polymeric TEMPO as the catholyte and a BODIPY copolymer as the anolyte. This battery featured a mean discharging voltage of 1.82 V and 100 consecutive charge/discharge cycles with 70 % retention of the initial discharge capacity. A second battery that featured two different BODIPY copolymers, one as the catholyte and a second as the anolyte, revealed a mean charging voltage of 2.06 V but only a mean discharging voltage of 1.28 V. Nevertheless, a stable battery cycling was observed for 90 consecutive charge/discharge cycles. A bipolar polymer, which can be used both in the catholyte and anolyte, has so far not been reported.

5. Photoelectrochemical Redox-Flow Batteries (Photo-RFBs)

RFBs are utilized as a buffer for intermittent electric energy. Electricity which is produced by wind power or solar energy is converted into chemical energy and stored for a certain amount of time. Photo-RFBs render this detour via electrical energy unnecessary, since light is directly stored as chemical energy. The development of highly efficient photoelectrodes and their integration into RFB technologies may result in the use of conventional photo-
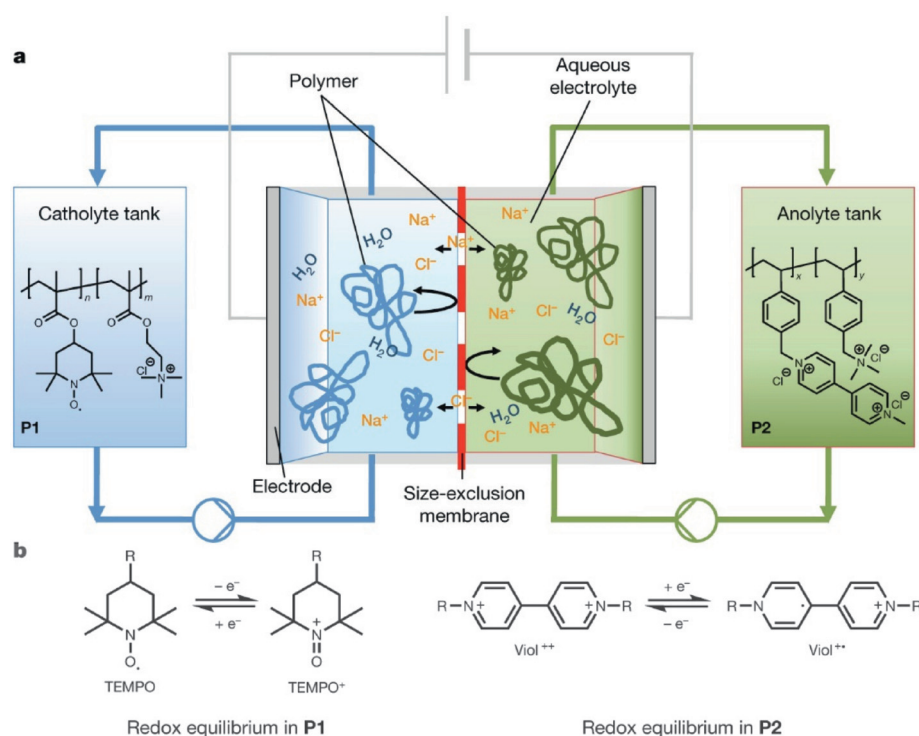

Figure 13. a) Schematic representation of a polymer-based RFB consisting of an electrochemical cell and two electrolyte reservoirs. The anolyte and catholyte cycle are separated by a semipermeable size-exclusion membrane, which retains the redox-active macromolecules while allowing small salt ions to pass. b) Fundamental electrode reactions of P1 (TEMPO radical) and P2 (viologen).[34]

voltaic systems and batteries becoming obsolete, thereby leading to a more cost-efficient and simpler all-in-one system.

The design of a photo-RFB is very similar to that of regular RFBs, but differs in the additional utilization of a photoelectrode, which is typically fabricated from conductive glass coated with a photocatalyst. A schematic representation is shown in Figure 15.
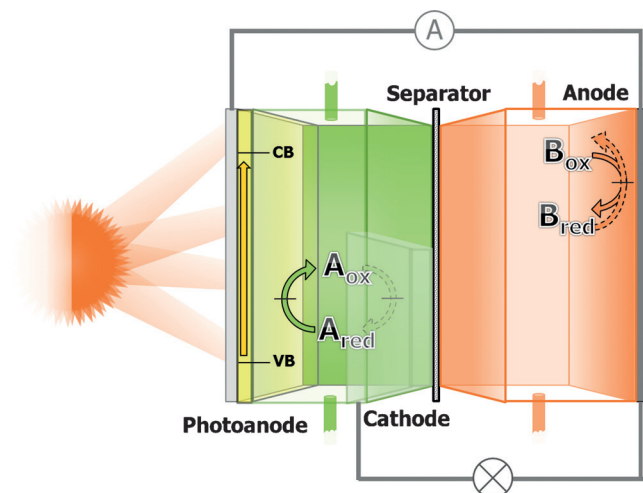

Figure 15. Schematic representation of a photoelectrochemical redox-flow battery.

The charging process is dependent on the photoanode. This electrode is mandatory for the light-harvesting process, as incident light generates electron-hole pairs, which induce the oxidation of the catholyte at the interface between the catholyte and photoanode.[188] Simultaneously, the anolyte is reduced by the transferred electron. The subsequent discharging procedure is the same as in regular RFBs.

5.1. Photoelectrochemical Redox-Flow Batteries with Asymmetric Electrolytes

The group of Gao and co-workers proposed this technology first and combined the classical dye-sensitized solar cell (DSSC, Grätzel cell) with the flow-battery technology.[189] FTO glass coated with TiO_2 and a ruthenium dye were utilized as the photoanode and the redox couple I_3^-/I^- as the catholyte. A Li^+ glass ceramic separator prevented electrolyte crossover and allowed charge equalization through the Li conductivity.

In a first publication, the anolyte contained decamethylferrocene, which led to an average discharging voltage of 0.33 V in the dark and a photocharging voltage of around 0.55 V. A maximum discharge capacity was reached with 53.3 mAh L^{-1}, which corresponds to a material utilization of 24% after an illumination time of 2400 s and 48% of the photocharge capacity.[189] In a second publication, the anolyte was replaced by an aqueous Li_2WO_4 solution.[190] This led to an elevated average discharging voltage of 0.45 V and a photocharge plateau voltage of 0.76 V.[190] In a third study,

quinoxaline derivatives were employed as the anode-active material and represent a first approach for the application of organic active materials in solar rechargeable RFBs.[191] As for the Li_2WO_4 system, charging voltages of 0.78 V and average discharging voltages of 0.45 V were achieved.

Gao et al. successfully demonstrated the possibility of combining a DSSC with a RFB. However, the presented systems have to overcome several challenges, since capacities, cell voltages, and applicable current densities are not competitive with state-of-the-art RFBs.

An improvement to these systems was reported by Wu et al., by using solid lithium as the anode.[192] In addition, guanidine thiocyanate and chenodeoxycholic acid were used as additives to improve the wettability on the hydrophobic dye-sensitized TiO_2 photoanode. The advantages of this system are the elevated charging and discharging voltages of 3.55 V and 3.35 V, respectively, and the ability to use a highly concentrated aqueous catholyte with a concentration of 2.0 M LiI. Consequently, the electrolyte revealed a theoretical capacity of 35.7 Ah L^{-1}. After 16.8 h, the battery was charged to 91% of its theoretical capacity and 25 charge/discharge cycles were demonstrated. The low photocharging rate is equally considered a drawback.

The photocharging capability of organic/inorganic RFBs with the anthraquinone derivative AQDS as the anode-active material and either ferrocyanide or bromide as the cathode-active material was demonstrated recently.[193, 194] Wedege et al. used a hematite photoanode annealed with polyaniline for the oxidation of ferrocyanide.[193] An unbiased photocharging was possible up to a state of charge of 12%.

Liao et al. used a dual silicon photoelectrochemical cell in an AQDS/bromide RFB.[194] The photocathode consisted of C/TiO_2/Ti/n$^+$ p-Si and the photoanode of Pt/p$^+$n-Si. A high conversion efficiency of 6% was achieved with these optimized photoelectrodes. The battery was self-charged to 0.8 V and a discharge capacity of 730 mAh L^{-1} was reached after photocharging for 2 h. The authors demonstrated constant capacity retention over ten consecutive charge/discharge cycles, which makes this system the most advanced photo-RFB so far.

5.2. Solar Chargeable All-Vanadium Redox-Flow Batteries

A few studies describe the solar charging of VRFBs with photoanodes in which TiO_2 and WO_3 as well as CdS are used.[195–198] However, electrical efficiencies are, to date, only moderate. Furthermore, a degradation of some photoanodes was observed in the highly acidic electrolyte.[197]

Current photo-RFB technologies are still in their infancy. Research should address the interaction between the photoelectrode and the active material by matching their redox potentials in relation to the conduction band of the semiconductor. Organic active materials can represent an ideal class of materials, since the redox potentials can be fine-tuned by variation of the substituents.

6. Conclusion and Future Challenges

Flow batteries are, in our opinion, the battery technology with the greatest potential to be one of the key elements in the energy transition to a sustainable electricity supply. The current redox couples and electrolytes in VRFB, Fe/Cr, and Zn/Br_2 systems represent only an intermediate step to nontoxic and noncorrosive electrolytes, which rely on organic or earth-abundant active materials. Improvements can be achieved by addressing the following challenges:

An increase in the energy density can be accomplished by utilizing redox-active materials with an elevated solubility of at least 2 M, which can be achieved by intelligent design of the molecules. Of particular interest are organic materials capable of transferring more than just one electron, as well as bipolar materials with a large difference between their redox potentials. The exact adjustment of the redox potential of the active material and the expanded potential window of water, by exploiting the overpotential of the electrode, can also significantly increase the energy density. Further approaches include the utilization of water-miscible liquid organic materials or decreasing the molar mass of a single molecule to decrease the solvent/active material mass ratio and, hence, to increase the solubility.

Suspension-based systems or ionic-liquid electrolytes have in fact the highest energy densities, but suffer enormously from minimum applicable current densities and their application is, therefore, not reasonable. For the same reason, the application of high-voltage systems, which require an organic solvent, is not desirable for large stationary battery systems. An elevated energy density would be desirable, as the space requirement of the battery and likewise the operating costs would decrease.

An increase in the current density can be achieved by accelerating the kinetic reactions on the electrodes. This can be realized by choosing appropriate electrode materials and/or their activation/modification. The modification of the electrodes is a completely novel approach, particularly for organic compounds. However, organic systems (e.g. quinones) already have advantages over vanadium-based systems in terms of their reaction kinetics. The applied membrane also has a significant impact on the current capability. In this context, the membrane should feature an ohmic resistance as low as possible and should allow a high counter-ion mobility. Membrane-free systems utilizing, for example, immiscible electrolytes could also lead to improvements.

Furthermore, the current density can be increased by reducing the viscosity of the electrolyte and thus enable accelerated charge-carrier transport. In regard to polymeric systems, this is achievable by utilizing (hyper)branched architectures.

An increase in the lifetime can be realized by the utilization of highly reversible redox couples, which undergo no side reactions and offer thousands of charge/discharge cycles. Therefore, systems that just transfer an electron but do not undergo a conformational change have the potential to be more stable. In addition, pH-sensitive molecules or redox reactions should be omitted. This includes the absence of functional groups prone to hydrolysis, such as esters. The temperature stability of organic redox couples in flow batteries at temperatures in the range of 50 to 70 °C has been barely investigated, but it is of high importance as organic compounds can undergo side reactions when a certain activation energy is exceeded.

The long life cycle of the electrodes can be improved by not utilizing strongly acidic conditions. The selectivity of the membrane also has a significant impact on the long-term retention of capacity. Highly selective membranes are required for the preservation of this performance characteristic. Membranes that are designed, in particular, for flow-battery applications are not commercially available. However, calculating a lifetime of 20 years with a capacity retention of 80 % and one charge/discharge cycle per day, the crossover of cathode and anode active material must not exceed 0.002 % per cycle. This illustrates why the development of bipolar organic active materials is highly attractive.

An increase in the overall system efficiency can be accomplished by expanding the temperature range in which no precipitation of either active material or supporting electrolyte occurs. This is also required for common metal-based RFBs (e.g. VRFBs, Fe/Cr, and Zn/Br_2) and would consequently reduce the energy demand for heating or cooling the electrolyte. The utilization of additives or the selection of active materials and supporting electrolytes with excellent solubility could allow this target to be met.

A decrease in the costs is an important, if not the most important, driving force to enable market penetration for RFBs. This goal can be accomplished by the utilization of organic materials or earth-abundant metals for the charge-storage process. Furthermore, the utilization of simple separators instead of complex ion-selective membranes would reduce the costs, likewise the utilization of water as solvent.

Concerning these requirements, key performance indicators such as levelized cost of energy ($\$\,MW^{-1}\,h^{-1}$) or costs per surface power density ($\$\,m^2\,W^{-1}$) seem to be reasonable assessment criteria. The duration of use has to be included in this calculation, as most RFBs have extended lifetimes compared to lead or lithium ion batteries.

In summary, research and development should focus on aqueous redox- and hybrid-flow batteries, which utilize organic active materials. In this case, highly soluble organic compounds, which can be produced with minimal effort in high yields, are favored to enable the efficient production of large-scale systems with capacities in the range of MW h. Additionally, a special focus on the system safety, in regard to the flammability and toxicity is required. In particular, for household-sized RFBs, which can be used in combination with decentralized roof-top photovoltaic electricity production, safe battery systems are absolute necessary. The HFB technology systems comprising a Zn anode should be investigated further, since this metal expands the usable voltage range in water and can be acquired at low cost.

Therefore, we suggest focusing on TEMPO as the organic cathode material for aqueous flow batteries. 4-HO-TEMPO can be purchased at prices of $\$5$–$6\,kg^{-1}$, and its solubility in water can be increased by alteration of the substituent in the 4-position. TEMPO has a high oxidation potential near the

upper limit of the potential window of water and reveals chemically reversible redox reactions in a pH range of 3 to 7. Viologen and anthraquinone species are suitable anode active materials which have good chemical reversibility and fast reaction kinetics. However, the solubility of either their uncharged state (e.g. AQDS) or charged state (e.g. dimethylviologen) has to be increased. Both molecules can be purchased at affordable costs, with dimethylviologen having the lower reduction potential at the bottom end of the water potential window.

We also see a backlog in membrane development, as most utilized membranes are designed for applications in fuel cells and not in RFBs. The utilization of biotechnology or extraction from renewable natural sources to obtain organic redox-active materials would further improve the environmental impact of RFBs.

Acknowledgements

How to cite: *Angew. Chem. Int. Ed.* **2017**, *56*, 686–711
Angew. Chem. **2017**, *129*, 702–729

[1] P. M. Vitousek, H. A. Mooney, J. Lubchenco, J. M. Melillo, *Science* **1997**, *277*, 494–499.

[2] P. Tans, R. Keeling, July 8, 2015 ed., NOAA, http://www.esrl.noaa.gov/gmd/ccgg/trends/, **2015**.

[3] S. Solomon, G.-K. Plattner, R. Knutti, P. Friedlingstein, *Proc. Natl. Acad. Sci. USA* **2009**, *106*, 1704–1709.

[4] P. M. Cox, R. A. Betts, C. D. Jones, S. A. Spall, I. J. Totterdell, *Nature* **2000**, *408*, 184–187.

[5] J. T. Houghton, L. G. M. Filho, B. A. Callander, N. Harris, A. Kattenberg, K. Maskell, *Climate Change 1995*: *The Science of Climate Change*, Cambridge Univ. Press, Cambridge, **1996**.

[6] M. S. Reddy, S. Basha, H. V. Joshi, B. Jha, *J. Hazard. Mater.* **2005**, *123*, 242–249.

[7] C. Tebert, Quecksilber-Emissionen aus Kohlekraftwerken, Ökopol GmbH, **2016**.

[8] I. Dincer, *Renewable Sustainable Energy Rev.* **2000**, *4*, 157–175.

[9] H. Lund, *Energy* **2007**, *32*, 912–919.

[10] G. Katata, M. Chino, T. Kobayashi, H. Terada, M. Ota, H. Nagai, M. Kajino, R. Draxler, M. C. Hort, A. Malo, T. Torii, Y. Sanada, *Atmos. Chem. Phys.* **2015**, *15*, 1029–1070.

[11] F. von Hippel, R. Ewing, R. Garwin, A. Macfarlane, *Nature* **2012**, *485*, 167–168.

[12] D. Cook, B. Davidsdottir, J. G. Petursson, *Renewable Sustainable Energy Rev.* **2015**, *49*, 211–220.

[13] D. M. Rosenberg, R. A. Bodaly, P. J. Usher, *Global Environ. Change* **1995**, *5*, 127–148.

[14] O. Edenhofer, K. Seyboth, F. Creutzig, S. Schlömer, *Annu. Rev. Environ. Resour.* **2013**, *38*, 169–200.

[15] S. Weitemeyer, D. Kleinhans, T. Vogt, C. Agert, *Renewable Energy* **2015**, *75*, 14–20.

[16] Z. Abdmouleh, R. A. M. Alammari, A. Gastli, *Renewable Sustainable Energy Rev.* **2015**, *45*, 249–262.

[17] P. Alstone, D. Gershenson, D. M. Kammen, *Nat. Clim. Change* **2015**, *5*, 305–314.

[18] P. Cappers, J. MacDonald, C. Goldman, O. Ma, *Energy Policy* **2013**, *62*, 1031–1039.

[19] B. Dunn, H. Kamath, J.-M. Tarascon, *Science* **2011**, *334*, 928–935.

[20] C. Budischak, D. Sewell, H. Thomson, L. Mach, D. E. Veron, W. Kempton, *J. Power Sources* **2013**, *225*, 60–74.

[21] P. Alotto, M. Guarnieri, F. Moro, *Renewable Sustainable Energy Rev.* **2014**, *29*, 325–335.

[22] P. K. Leung, C. Ponce-de-León, C. T. J. Low, F. C. Walsh, *Electrochim. Acta* **2011**, *56*, 6536–6546.

[23] A. Weber, M. Mench, J. Meyers, P. Ross, J. Gostick, Q. Liu, *J. Appl. Electrochem.* **2011**, *41*, 1137–1164.

[24] J.-Y. Chen, C.-L. Hsieh, N.-Y. Hsu, Y.-S. Chou, Y.-S. Chen, *Energies* **2014**, *7*, 5863.

[25] K. Bromberger, J. Kaunert, T. Smolinka, *Energy Technol.* **2014**, *2*, 64–76.

[26] S. Muench, A. Wild, C. Friebe, B. Haeupler, T. Janoschka, U. S. Schubert, *Chem. Rev.* **2016**, *116*, 9438–9484.

[27] R. Darling, K. Gallagher, W. Xie, L. Su, F. Brushett, *J. Electrochem. Soc.* **2016**, *163*, A5029–A5040.

[28] R. A. Potash, J. R. McKone, S. Conte, H. D. Abruña, *J. Electrochem. Soc.* **2016**, *163*, A338–A344.

[29] J. Cheng, L. Zhang, Y.-S. Yang, Y.-H. Wen, G.-P. Cao, X.-D. Wang, *Electrochem. Commun.* **2007**, *9*, 2639–2642.

[30] W. A. Braff, M. Z. Bazant, C. R. Buie, *Nat. Commun.* **2013**, *4*, 2346.

[31] X. Li, H. Zhang, Z. Mai, H. Zhang, I. Vankelecom, *Energy Environ. Sci.* **2011**, *4*, 1147–1160.

[32] J. Winsberg, T. Janoschka, S. Morgenstern, S. Muench, T. Hagemann, G. Hauffman, J.-F. Gohy, M. D. Hager, U. S. Schubert, *Adv. Mater.* **2016**, *28*, 2238–2243.

[33] J. Winsberg, S. Muench, T. Hagemann, T. Janoschka, S. Morgenstern, M. Billing, F. H. Schacher, G. Hauffman, J.-F. Gohy, S. Hoeppener, M. D Hager, U. S. Schubert, *Polym. Chem.* **2016**, *7*, 1711–1718.

[34] T. Janoschka, N. Martin, U. Martin, C. Friebe, S. Morgenstern, H. Hiller, M. D. Hager, U. S. Schubert, *Nature* **2015**, *527*, 78–81.

[35] Y. Zhao, S. Si, C. Liao, *J. Power Sources* **2013**, *241*, 449–453.

[36] G. Nagarjuna, J. Hui, K. J. Cheng, T. Lichtenstein, M. Shen, J. S. Moore, J. Rodríguez-López, *J. Am. Chem. Soc.* **2014**, *136*, 16309–16316.

[37] L. W. Hruska, R. F. Savinell, *J. Electrochem. Soc.* **1981**, *128*, 18–25.

[38] Z. Yuan, X. Zhu, M. Li, W. Lu, X. Li, H. Zhang, *Angew. Chem. Int. Ed.* **2016**, *55*, 3058–3062; *Angew. Chem.* **2016**, *128*, 3110–3114.

[39] J. Drillkens, D. Schulte, D. U. Sauer, *ECS Trans.* **2010**, *28*, 167–177.

[40] M. Vijayakumar, M. S. Bhuvaneswari, P. Nachimuthu, B. Schwenzer, S. Kim, Z. Yang, J. Liu, G. L. Graff, S. Thevuthasan, J. Hu, *J. Membr. Sci.* **2011**, *366*, 325–334.

[41] K. Takechi, Y. Kato, Y. Hase, *Adv. Mater.* **2015**, *27*, 2501–2506.

[42] X. Sun, T. Souier, M. Chiesa, A. Vassallo, *Electrochim. Acta* **2014**, *148*, 104–110.

[43] G. Nikiforidis, W. A. Daoud, *J. Electrochem. Soc.* **2015**, *162*, A809–A819.

[44] P. Trogadas, O. O. Taiwo, B. Tjaden, T. P. Neville, S. Yun, J. Parrondo, V. Ramani, M.-O. Coppens, D. J. L. Brett, P. R. Shearing, *Electrochem. Commun.* **2014**, *48*, 155–159.

[45] H. Liu, Q. Xu, C. Yan, *Electrochem. Commun.* **2013**, *28*, 58–62.

[46] P. K. Leung, C. Ponce-de-León, F. J. Recio, P. Herrasti, F. C. Walsh, *J. Appl. Electrochem.* **2014**, *44*, 1025–1035.

[47] B. Li, M. Gu, Z. Nie, X. Wei, C. Wang, V. Sprenkle, W. Wang, *Nano Lett.* **2014**, *14*, 158–165.

[48] Z. González, A. Sánchez, C. Blanco, M. Granda, R. Menéndez, R. Santamaría, *Electrochem. Commun.* **2011**, *13*, 1379–1382.

[49] W. H. Wang, X. D. Wang, *Electrochim. Acta* **2007**, *52*, 6755–6762.

[50] Z. He, L. Dai, S. Liu, L. Wang, C. Li, *Electrochim. Acta* **2015**, *176*, 1434–1440.

[51] A. M. Pezeshki, J. T. Clement, G. M. Veith, T. A. Zawodzinski, M. M. Mench, *J. Power Sources* **2015**, *294*, 333–338.

[52] G. Nikiforidis, W. A. Daoud, *Electrochim. Acta* **2015**, *168*, 394–402.

[53] G. Nikiforidis, Y. Xiang, W. A. Daoud, *Electrochim. Acta* **2015**, *157*, 274–281.

[54] J.-Z. Chen, W.-Y. Liao, W.-Y. Hsieh, C.-C. Hsu, Y.-S. Chen, *J. Power Sources* **2015**, *274*, 894–898.

[55] T.-M. Tseng, R.-H. Huang, C.-Y. Huang, K.-L. Hsueh, F.-S. Shieu, *J. Electrochem. Soc.* **2013**, *160*, A1269–A1275.

[56] K. J. Kim, M.-S. Park, Y.-J. Kim, J. H. Kim, S. X. Dou, M. Skyllas-Kazacos, *J. Mater. Chem. A* **2015**, *3*, 16913–16933.

[57] Y. Munaiah, S. Suresh, S. Dheenadayalan, V. K. Pillai, P. Ragupathy, *J. Phys. Chem. C* **2014**, *118*, 14795–14804.

[58] J.-H. Kim, K. J. Kim, M.-S. Park, N. J. Lee, U. Hwang, H. Kim, Y.-J. Kim, *Electrochem. Commun.* **2011**, *13*, 997–1000.

[59] P. K. Leung, C. Ponce-de-León, C. T. J. Low, A. A. Shah, F. C. Walsh, *J. Power Sources* **2011**, *196*, 5174–5185.

[60] M. Rychcik, M. Skyllas-Kazacos, *J. Power Sources* **1987**, *19*, 45–54.

[61] D. J. Suárez, Z. González, C. Blanco, M. Granda, R. Menéndez, R. Santamaría, *ChemSusChem* **2014**, *7*, 914–918.

[62] M. Skyllas-Kazacos, M. H. Chakrabarti, S. A. Hajimolana, F. S. Mjalli, M. Saleem, *J. Electrochem. Soc.* **2011**, *158*, R55–R79.

[63] P. Leung, X. Li, C. Ponce-de-León, L. Berlouis, C. T. J. Low, F. C. Walsh, *RSC Adv.* **2012**, *2*, 10125–10156.

[64] D. D. Banham-Hall, G. A. Taylor, C. A. Smith, M. R. Irving, *IEEE Trans. Power Syst.* **2012**, *27*, 1690–1697.

[65] P. Denholm, M. O'Connell, G. Brinkman, J. Jorgenson, *Overgeneration from Solar Energy in California: A Field Guide to the Duck Chart*, National Renewable Energy Laboratory, **2015**.

[66] H. Wirth, *Recent Facts about Photovoltaics in Germany*, Fraunhofer Institut for Solar Energy Systems ISE, **2016**.

[67] B. Burger, *Stromerzeugung aus Solar- und Windenergie im Jahr 2014*, Fraunhofer Institut for Solar Energy Systems ISE, **2015**.

[68] Z. Yang, J. Zhang, M. C. W. Kintner-Meyer, X. Lu, D. Choi, J. P. Lemmon, J. Liu, *Chem. Rev.* **2011**, *111*, 3577–3613.

[69] J. A. Short, D. G. Infield, L. L. Freris, *IEEE Trans. Power Syst.* **2007**, *22*, 1284–1293.

[70] S. Roe, C. Menictas, M. Skyllas-Kazacos, *J. Electrochem. Soc.* **2016**, *163*, A5023–A5028.

[71] W. Wang, Q. Luo, B. Li, X. Wei, L. Li, Z. Yang, *Adv. Funct. Mater.* **2013**, *23*, 970–986.

[72] P. Poizot, F. Dolhem, *Energy Environ. Sci.* **2011**, *4*, 2003–2019.

[73] C.-J. Yang, R. B. Jackson, *Renewable Sustainable Energy Rev.* **2011**, *15*, 839–844.

[74] K. Gong, X. Ma, K. M. Conforti, K. J. Kuttler, J. B. Grunewald, K. L. Yeager, M. Z. Bazant, S. Gu, Y. Yan, *Energy Environ. Sci.* **2015**, *8*, 2941–2945.

[75] R. M. Darling, K. G. Gallagher, J. A. Kowalski, S. Ha, F. R. Brushett, *Energy Environ. Sci.* **2014**, *7*, 3459–3477.

[76] A. Crawford, V. Viswanathan, D. Stephenson, W. Wang, E. Thomsen, D. Reed, B. Li, P. Balducci, M. Kintner-Meyer, V. Sprenkle, *J. Power Sources* **2015**, *293*, 388–399.

[77] V. Viswanathan, A. Crawford, D. Stephenson, S. Kim, W. Wang, B. Li, G. Coffey, E. Thomsen, G. Graff, P. Balducci, M. Kintner-Meyer, V. Sprenkle, *J. Power Sources* **2014**, *247*, 1040–1051.

[78] B. Huskinson, M. P. Marshak, C. Suh, S. Er, M. R. Gerhardt, C. J. Galvin, X. Chen, A. Aspuru-Guzik, R. G. Gordon, M. J. Aziz, *Nature* **2014**, *505*, 195–198.

[79] X. Zhang, L. Yang, Y. Li, H. Li, W. Wang, B. Ye, *Environ. Monit. Assess.* **2012**, *184*, 2261–2273.

[80] Y. Zhao, Y. Ding, Y. Li, L. Peng, H. R. Byon, J. B. Goodenough, G. Yu, *Chem. Soc. Rev.* **2015**, *44*, 7968–7996.

[81] G. L. Soloveichik, *Chem. Rev.* **2015**, *115*, 11533–11558.

[82] M. Skyllas-Kazacos, L. Cao, M. Kazacos, N. Kausar, A. Mousa, *ChemSusChem* **2016**, *9*, 1521–1543.

[83] J. Noack, N. Roznyatovskaya, T. Herr, P. Fischer, *Angew. Chem. Int. Ed.* **2015**, *54*, 9776–9809; *Angew. Chem.* **2015**, *127*, 9912–9947.

[84] W. Kangro, DE914264, **1949**.

[85] W. Kangro, H. Pieper, *Electrochim. Acta* **1962**, *7*, 435–448.

[86] W. Kangro, DE1006479, **1957**.

[87] N. H. Hagedorn, NASA TM-83677 Redox Storage System, **1984**.

[88] M. Skyllas-Kazacos, R. G. Robins, AU 575247, **1986**.

[89] M. Skyllas-Kazacos, M. Rychcik, R. G. Robins, A. G. Fane, *J. Electrochem. Soc.* **1986**, *133*, 1057–1058.

[90] C. S. Bradley, US 312802, **1885**.

[91] D. J. Eustace, US 4064324, **1977**.

[92] D. Linden, T. B. Reddy, *Handbook of Batteries*, McGraw-Hill, New York, **2002**.

[93] M. d. Rossi, US 3738870, **1973**.

[94] K. J. Cathro, K. Cedzynska, D. C. Constable, P. M. Hoobin, *J. Power Sources* **1986**, *18*, 349–370.

[95] R. Clarke, B. Dougherty, S. Harrison, P. Millington, S. Mohanta, US 0202925 A1, **2004**.

[96] M. H. Chakrabarti, R. A. W. Dryfe, E. P. L. Roberts, *Electrochim. Acta* **2007**, *52*, 2189–2195.

[97] M. H. Chakrabarti, E. P. L. Roberts, C. Bae, M. Saleem, *Energy Convers. Manage.* **2011**, *52*, 2501–2508.

[98] T. Yamamura, Y. Shiokawa, H. Yamana, H. Moriyama, *Electrochim. Acta* **2002**, *48*, 43–50.

[99] F.-Q. Xue, Y.-L. Wang, W.-H. Wang, X.-D. Wang, *Electrochim. Acta* **2008**, *53*, 6636–6642.

[100] L. Sanz, D. Lloyd, E. Magdalena, J. Palma, K. Kontturi, *J. Power Sources* **2014**, *268*, 121–128.

[101] D. Pletcher, R. Wills, *Phys. Chem. Chem. Phys.* **2004**, *6*, 1779–1785.

[102] R. F. Savinell, C. C. Liu, R. T. Galasco, S. H. Chiang, J. F. Coetzee, *J. Electrochem. Soc.* **1979**, *126*, 357–360.

[103] J. Pan, Y. Sun, J. Cheng, Y. Wen, Y. Yang, P. Wan, *Electrochem. Commun.* **2008**, *10*, 1226–1229.

[104] M. Duduta, B. Ho, V. C. Wood, P. Limthongkul, V. E. Brunini, W. C. Carter, Y.-M. Chiang, *Adv. Energy Mater.* **2011**, *1*, 511–516.

[105] Y. Zhao, H. R. Byon, *Adv. Energy Mater.* **2013**, *3*, 1630–1635.

[106] Y. Yang, G. Zheng, Y. Cui, *Energy Environ. Sci.* **2013**, *6*, 1552–1558.

[107] N. Singh, E. W. McFarland, *J. Power Sources* **2015**, *288*, 187–198.

[108] K. T. Cho, P. Ridgway, A. Z. Weber, S. Haussener, V. Battaglia, V. Srinivasan, *J. Electrochem. Soc.* **2012**, *159*, A1806–A1815.

[109] L. Li, S. Kim, W. Wang, M. Vijayakumar, Z. Nie, B. Chen, J. Zhang, G. Xia, J. Hu, G. Graff, J. Liu, Z. Yang, *Adv. Energy Mater.* **2011**, *1*, 394–400.

[110] B. Li, Z. Nie, M. Vijayakumar, G. Li, J. Liu, V. Sprenkle, W. Wang, *Nat. Commun.* **2015**, *6*, 6303.

[111] H. Chen, Q. Zou, Z. Liang, H. Liu, Q. Li, Y.-C. Lu, *Nat. Commun.* **2015**, *6*, 5877.

[112] S. Mubeen, Y.-s. Jun, J. Lee, E. W. McFarland, *ACS Appl. Mater. Interfaces* **2016**, *8*, 1759–1765.

[113] Q. Huang, J. Yang, C. B. Ng, C. Jia, Q. Wang, *Energy Environ. Sci.* **2016**, *9*, 917–931.

[114] S. Monaco, F. Soavi, M. Mastragostino, *J. Phys. Chem. Lett.* **2013**, *4*, 1379–1382.

[115] J. G. Austing, C. N. Kirchner, E.-M. Hammer, L. Komsiyska, G. Wittstock, *J. Power Sources* **2015**, *273*, 1163–1170.

[116] J. G. Austing, C. N. Kirchner, L. Komsiyska, G. Wittstock, *J. Power Sources* **2016**, *306*, 692–701.

[117] C. Menictas, M. Skyllas-Kazacos, *J. Appl. Electrochem.* **2011**, *41*, 1223–1232.

[118] H. Kaneko, A. Negishi, K. Nozaki, K. Sato, M. Nakajima, US 5318865A, **1994**.

[119] J. Noack, C. Cremers, D. Bayer, J. Tübke, K. Pinkwart, *J. Power Sources* **2014**, *253*, 397–403.

[120] X. Wei, G.-G. Xia, B. Kirby, E. Thomsen, B. Li, Z. Nie, G. G. Graff, J. Liu, V. Sprenkle, W. Wang, *J. Electrochem. Soc.* **2016**, *163*, A5150–A5153.

[121] A. K. Manohar, K. M. Kim, E. Plichta, M. Hendrickson, S. Rawlings, S. R. Narayanan, *J. Electrochem. Soc.* **2016**, *163*, A5118–A5125.

[122] M. Armand, J. M. Tarascon, *Nature* **2008**, *451*, 652–657.

[123] C. J. Barnhart, S. M. Benson, *Energy Environ. Sci.* **2013**, *6*, 1083–1092.

[124] Q. Lai, H. Zhang, X. Li, L. Zhang, Y. Cheng, *J. Power Sources* **2013**, *235*, 1–4.

[125] Y. H. Wen, H. M. Zhang, P. Qian, H. T. Zhou, P. Zhao, B. L. Yi, Y. S. Yang, *J. Electrochem. Soc.* **2006**, *153*, A929–A934.

[126] X. Wei, W. Xu, M. Vijayakumar, L. Cosimbescu, T. Liu, V. Sprenkle, W. Wang, *Adv. Mater.* **2014**, *26*, 7649–7653.

[127] Q. Chen, M. R. Gerhardt, L. Hartle, M. J. Aziz, *J. Electrochem. Soc.* **2016**, *163*, A5010–A5013.

[128] B. Yang, L. Hoober-Burkhardt, F. Wang, G. K. S. Prakash, S. R. Narayanan, *J. Electrochem. Soc.* **2014**, *161*, A1371–A1380.

[129] Z. Li, S. Li, S. Liu, K. Huang, D. Fang, F. Wang, S. Peng, *Electrochem. Solid-State Lett.* **2011**, *14*, A171–A173.

[130] A. J. Bard, L. R. Faulkner, *Electrochemical Methods*, 2nd ed., Wiley, New York, **2001**.

[131] Y. Xu, Y. Wen, J. Cheng, G. Cao, Y. Yang, *Electrochem. Commun.* **2009**, *11*, 1422–1424.

[132] S. H. Oh, C. W. Lee, D. H. Chun, J. D. Jeon, J. Shim, K. H. Shin, J. H. Yang, *J. Mater. Chem. A* **2014**, *2*, 19994–19998.

[133] Y. Xu, Y.-H. Wen, J. Cheng, G.-P. Cao, Y.-S. Yang, *Electrochim. Acta* **2010**, *55*, 715–720.

[134] J. Huang, L. Cheng, R. S. Assary, P. Wang, Z. Xue, A. K. Burrell, L. A. Curtiss, L. Zhang, *Adv. Energy Mater.* **2015**, *5*, 1401782.

[135] T. Liu, X. Wei, Z. Nie, V. Sprenkle, W. Wang, *Adv. Energy Mater.* **2016**, *6*, 1501449.

[136] X. Wei, W. Xu, J. Huang, L. Zhang, E. Walter, C. Lawrence, M. Vijayakumar, W. A. Henderson, T. Liu, L. Cosimbescu, B. Li, V. Sprenkle, W. Wang, *Angew. Chem. Int. Ed.* **2015**, *54*, 8684–8687; *Angew. Chem.* **2015**, *127*, 8808–8811.

[137] Y. K. Zeng, T. S. Zhao, L. An, X. L. Zhou, L. Wei, *J. Power Sources* **2015**, *300*, 438–443.

[138] W. Wang, W. Xu, L. Cosimbescu, D. Choi, L. Li, Z. Yang, *Chem. Commun.* **2012**, *48*, 6669–6671.

[139] H. Alt, H. Binder, A. Köhling, G. Sandstede, *Electrochim. Acta* **1972**, *17*, 873–887.

[140] T. Le Gall, K. H. Reiman, M. C. Grossel, J. R. Owen, *J. Power Sources* **2003**, *119–121*, 316–320.

[141] Z. Song, H. Zhan, Y. Zhou, *Chem. Commun.* **2009**, 448–450.

[142] Z. Lei, W. Wei-kun, W. An-bang, Y. Zhong-bao, C. Shi, Y. Yu-sheng, *J. Electrochem. Soc.* **2011**, *158*, A991–A996.

[143] W. Xu, A. Read, P. K. Koech, D. Hu, C. Wang, J. Xiao, A. B. Padmaperuma, G. L. Graff, J. Liu, J.-G. Zhang, *J. Mater. Chem.* **2012**, *22*, 4032–4039.

[144] S. P. Ong, V. L. Chevrier, G. Hautier, A. Jain, C. Moore, S. Kim, X. Ma, G. Ceder, *Energy Environ. Sci.* **2011**, *4*, 3680–3688.

[145] J. E. Bachman, L. A. Curtiss, R. S. Assary, *J. Phys. Chem. A* **2014**, *118*, 8852–8860.

[146] M. Quan, D. Sanchez, M. F. Wasylkiw, D. K. Smith, *J. Am. Chem. Soc.* **2007**, *129*, 12847–12856.

[147] K. Lin, Q. Chen, M. R. Gerhardt, L. Tong, S. B. Kim, L. Eisenach, A. W. Valle, D. Hardee, R. G. Gordon, M. J. Aziz, M. P. Marshak, *Science* **2015**, *349*, 1529–1532.

[148] H. Nishide, S. Iwasa, Y.-J. Pu, T. Suga, K. Nakahara, M. Satoh, *Electrochim. Acta* **2004**, *50*, 827–831.

[149] Y. Liang, Z. Tao, J. Chen, *Adv. Energy Mater.* **2012**, *2*, 742–769.

[150] T. Janoschka, M. D. Hager, U. S. Schubert, *Adv. Mater.* **2012**, *24*, 6397–6409.

[151] M. C. Krishna, D. A. Grahame, A. Samuni, J. B. Mitchell, A. Russo, *Proc. Natl. Acad. Sci. USA* **1992**, *89*, 5537–5541.

[152] A. E. S. Sleightholme, A. A. Shinkle, Q. Liu, Y. Li, C. W. Monroe, L. T. Thompson, *J. Power Sources* **2011**, *196*, 5742–5745.

[153] A. A. Shinkle, A. E. S. Sleightholme, L. D. Griffith, L. T. Thompson, C. W. Monroe, *J. Power Sources* **2012**, *206*, 490–496.

[154] T. Herr, J. Noack, P. Fischer, J. Tübke, *Electrochim. Acta* **2013**, *113*, 127–133.

[155] G. Oriji, Y. Katayama, T. Miura, *Electrochim. Acta* **2004**, *49*, 3091–3095.

[156] Y. Wen, H. Zhang, P. Qian, P. Zhao, H. Zhou, B. Yi, *Acta Phys.-Chim. Sin.* **2006**, *22*, 403–408.

[157] E. Sum, M. Rychcik, M. Skyllas-Kazacos, *J. Power Sources* **1985**, *16*, 85–95.

[158] E. Sum, M. Skyllas-Kazacos, *J. Power Sources* **1985**, *15*, 179–190.

[159] F. R. Brushett, J. T. Vaughey, A. N. Jansen, *Adv. Energy Mater.* **2012**, *2*, 1390–1396.

[160] L. Su, M. Ferrandon, J. A. Kowalski, J. T. Vaughey, F. R. Brushett, *J. Electrochem. Soc.* **2014**, *161*, A1905–A1914.

[161] S. Zhang, X. Li, D. Chu, *Electrochim. Acta* **2016**, *190*, 737–743.

[162] J. Huang, L. Su, J. A. Kowalski, J. L. Barton, M. Ferrandon, A. K. Burrell, F. R. Brushett, L. Zhang, *J. Mater. Chem. A* **2015**, *3*, 14971–14976.

[163] L. Zhang, Z. Zhang, P. C. Redfern, L. A. Curtiss, K. Amine, *Energy Environ. Sci.* **2012**, *5*, 8204–8207.

[164] Lutfullah, H. S. Dunsmore, R. Paterson, *J. Chem. Soc. Faraday Trans. 1* **1976**, *72*, 495–503.

[165] S. Wu, Y. Zhao, D. Li, Y. Xia, S. Si, *J. Power Sources* **2015**, *275*, 305–311.

[166] T. Sukegawa, I. Masuko, K. Oyaizu, H. Nishide, *Macromolecules* **2014**, *47*, 8611–8617.

[167] H. D. Inerowicz, W. Li, I. Persson, *J. Chem. Soc. Faraday Trans.* **1994**, *90*, 2223–2234.

[168] B. Huskinson, M. P. Marshak, M. R. Gerhardt, M. J. Aziz, *ECS Trans.* **2014**, *61*, 27–30.

[169] M. L. Perry, R. M. Darling, R. Zaffou, *ECS Trans.* **2013**, *53*, 7–16.

[170] Q. Chen, L. Eisenach, M. J. Aziz, *J. Electrochem. Soc.* **2016**, *163*, A5057–A5063.

[171] X. Li, *Electrochim. Acta* **2015**, *170*, 98–109.

[172] D. Chu, X. Li, S. Zhang, *Electrochim. Acta* **2016**, *190*, 434–445.

[173] P. G. Rasmussen, US 8080327 B1, **2011**.

[174] W. Duan, R. S. Vemuri, J. D. Milshtein, S. Laramie, R. D. Dmello, J. Huang, L. Zhang, D. Hu, M. Vijayakumar, W. Wang, J. Liu, R. M. Darling, L. Thompson, K. Smith, J. S. Moore, F. R. Brushett, X. Wei, *J. Mater. Chem. A* **2016**, *4*, 5448–5456.

[175] J. H. Osiecki, E. F. Ullman, *J. Am. Chem. Soc.* **1968**, *90*, 1078–1079.

[176] T. Sukegawa, A. Kai, K. Oyaizu, H. Nishide, *Macromolecules* **2013**, *46*, 1361–1367.

[177] J. Lee, E. Lee, S. Kim, G. S. Bang, D. A. Shultz, R. D. Schmidt, M. D. E. Forbes, H. Lee, *Angew. Chem. Int. Ed.* **2011**, *50*, 4414–4418; *Angew. Chem.* **2011**, *123*, 4506–4510.

[178] R. Ziessel, G. Ulrich, R. C. Lawson, L. Echegoyen, *J. Mater. Chem.* **1999**, *9*, 1435 – 1448.

[179] E. Coronado, C. Gimenez-Saiz, M. Nicolas, F. M. Romero, E. Rusanov, H. Stoeckli-Evans, *New J. Chem.* **2003**, *27*, 490 – 497.

[180] Y. Nakano, T. Yagyu, T. Hirayama, A. Ito, K. Tanaka, *Polyhedron* **2005**, *24*, 2141 – 2147.

[181] A. Caneschi, D. Gatteschi, N. Lalioti, C. Sangregorio, R. Sessoli, G. Venturi, A. Vindigni, A. Rettori, M. G. Pini, M. A. Novak, *Angew. Chem. Int. Ed.* **2001**, *40*, 1760 – 1763; *Angew. Chem.* **2001**, *113*, 1810 – 1813.

[182] S. Y. Zhou, X. Li, T. Li, L. Tian, Z. Y. Liu, X. G. Wang, *RSC Adv.* **2015**, *5*, 17131 – 17139.

[183] L.-L. Li, S. Liu, Y. Zhang, W. Shi, P. Cheng, *Dalton Trans.* **2015**, *44*, 6118 – 6125.

[184] A. P. Kaur, N. E. Holubowitch, S. Ergun, C. F. Elliott, S. A. Odom, *Energy Technol.* **2015**, *3*, 446.

[185] E. Fritz-Langhals, *Org. Process Res. Dev.* **2005**, *9*, 577 – 582.

[186] T. Janoschka, S. Morgenstern, H. Hiller, C. Friebe, K. Wolkersdörfer, B. Häupler, M. D. Hager, U. S. Schubert, *Polym. Chem.* **2015**, *6*, 7801 – 7811.

[187] J. Winsberg, T. Hagemann, S. Muench, C. Friebe, B. Häupler, T. Janoschka, S. Morgenstern, M. D. Hager, U. S. Schubert, *Chem. Mater.* **2016**, *28*, 3401 – 3405.

[188] D. Sengupta, P. Das, B. Mondal, K. Mukherjee, *Renewable Sustainable Energy Rev.* **2016**, *60*, 356 – 376.

[189] P. Liu, Y.-l. Cao, G.-R. Li, X.-P. Gao, X.-P. Ai, H.-X. Yang, *ChemSusChem* **2013**, *6*, 802 – 806.

[190] N. F. Yan, G. R. Li, X. P. Gao, *J. Mater. Chem. A* **2013**, *1*, 7012 – 7015.

[191] N. F. Yan, G. R. Li, X. P. Gao, *J. Electrochem. Soc.* **2014**, *161*, A736 – A741.

[192] M. Yu, W. D. McCulloch, D. R. Beauchamp, Z. Huang, X. Ren, Y. Wu, *J. Am. Chem. Soc.* **2015**, *137*, 8332 – 8335.

[193] K. Wedege, J. Azevedo, A. Khataee, A. Bentien, A. Mendes, *Angew. Chem. Int. Ed.* **2016**, *55*, 7142 – 7147; *Angew. Chem.* **2016**, *128*, 7258 – 7263.

[194] S. Liao, X. Zong, B. Seger, T. Pedersen, T. Yao, C. Ding, J. Shi, J. Chen, C. Li, *Nat. Commun.* **2016**, *7*, 11474.

[195] Z. Wei, D. Liu, C. Hsu, F. Liu, *Electrochem. Commun.* **2014**, *45*, 79 – 82.

[196] D. Liu, Z. Wei, C.-j. Hsu, Y. Shen, F. Liu, *Electrochim. Acta* **2014**, *136*, 435 – 441.

[197] J. Azevedo, T. Seipp, J. Burfeind, C. Sousa, A. Bentien, J. P. Araújo, A. Mendes, *Nano Energy* **2016**, *22*, 396 – 405.

[198] Z. Peimanifard, S. Rashid-Nadimi, *J. Power Sources* **2015**, *300*, 395 – 401.

[199] T. Janoschka, N. Martin, M. D. Hager, U. S. Schubert, *Angew. Chem. Int. Ed.* **2016**, DOI: 10.1002/anie.201606472; *Angew. Chem.* **2016**, DOI: 10.1002/ange.201606472.

[200] J. Winsberg, C. Stolze, S. Muench, F. Liedl, M. D. Hager, U. S. Schubert, *ACS Energy Lett.* **2016**, DOI: 10.1021/acsenergylett.6b00413.